TIGHT BINDING BOOK

Cambridge Physical Tracts

ELECTRON OPTICS

CAMBRIDGE
UNIVERSITY PRESS
LONDON: BENTLEY HOUSE

NEW YORK, TORONTO, BOMBAY
CALCUTTA, MADRAS: MACMILLAN

TOKYO: MARUZEN COMPANY LTD

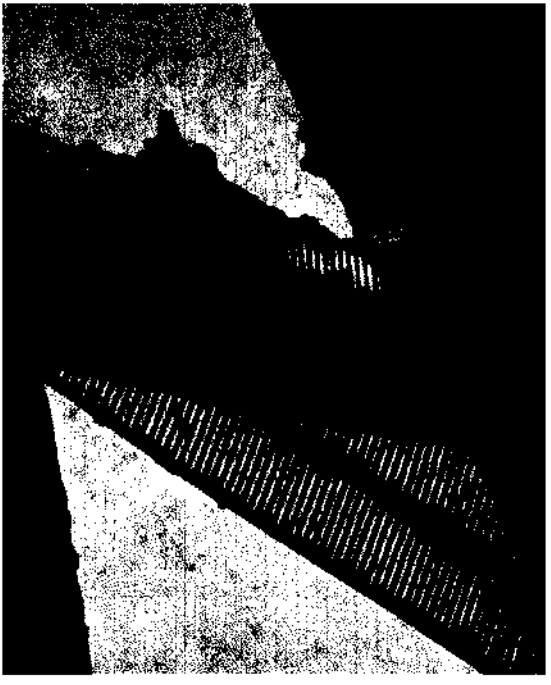

10^{-4} cm.

Electron-optical micro-photograph of diatoms. See p. 89.

0·1 mm.

α γ

Electron-optical micro-photograph of emission from an iron strip activated with Sr and Ba. See p. 85.

ELECTRON OPTICS

by

THE RESEARCH STAFF OF ELECTRIC AND MUSICAL INDUSTRIES LIMITED

Compiled and written
by

OTTO KLEMPERER

CAMBRIDGE
AT THE UNIVERSITY PRESS
1939

PRINTED IN GREAT BRITAIN

GENERAL PREFACE

It is the aim of these tracts to provide authoritative accounts of subjects of topical physical interest written by those actively engaged in research. Each author is encouraged to adopt an individualistic outlook and to write the tract from his own point of view without necessarily making it "complete'* by the inclusion of references to all other workers or to all allied subjects; it is hoped that the tracts may present such surveys of subjects as the authors might give in a short course of specialised lectures.

By this means readers will be provided with accounts of those subjects which are advancing so rapidly that a full-length book would be out of place. From time to time it is hoped to issue new editions of tracts dealing with subjects in which the advance is most rapid.

M. L. O.
J. A. R.

*** Notes in round brackets in the text, as, for example, (A. I), refer to the list of the literature.**

PREFACE

The aim of this tract is to give a concise account of the most important principles, methods, and applications of geometrical electron optics. The tract should be intelligible to the advanced student of experimental physics and to the research worker who has not specialised either in geometrical optics or in electron physics. Thus it may be studied without any particular knowledge except that of the fundamentals of general physics.

After some introductory notes given in Chapter I, Chapters II and vi deal with an introduction to the principal conceptions of first order and third order geometrical optics, and the meaning of these conceptions is elucidated by the example of the electron lens. In Chapter III, the plotting of electric fields and the tracing of rays through these fields is explained in detail. A clear understanding of this subject will open the way for a mental apprehension of the electron optical method. Chapter iv deals with the characteristics of some special types of electric lenses, whilst a general outline of the characteristics of magnetic lenses is given in Chapter v.

Finally, in Chapter vII, some practical applications of electron optics are described. It will be seen that the subject of electron optics is not only of academic interest but that it also has important technical applications. In this way the tract might help to introduce physicists and engineers to this subject if they start working in the new industries which are based on the electron optical science.

The physical facts compiled in this tract are taken from the numerous papers of the literature comprising many hundred investigations on electron optical subjects. A substantial fraction of the content represents a synopsis of reports of research work performed in the E.M.L Research Laboratories.

I would like to express my thanks to Mr I. Shoenberg, director of research of Electric and Musical Industries Ltd., for his encouragement to publish these pages and I owe an acknowledgment to Mr G. E. Condliffe and to the staff of the E.M.L Research Department. I am especially indebted to Dr L. F. Broadway and to Dr W. D. Wright, who both read the manuscript and made several suggestions for its improvement, and also to Mr J. A. Ratcliffe for help with the final wording.

OTTO KLEMPERER
70, *Syke Ings*
Iver, Bucks.

ELECTRIC AND MUSICAL
INDUSTRIES,
HAYES, MIDDLESEX

December, 1938

Chapter I

HISTORICAL INTRODUCTION. THE FUNDAMENTAL PRINCIPLES OF ELECTRON OPTICS

Electron optics is a relatively new field of science, although neither the method, nor the subject which is attacked by the method, is new. The results however are striking, new, and extremely useful. The method is that of geometrical optics, which was developed by several generations of physicists. The motion of electrons has been studied in many experimental and theoretical investigations; but in all these the mechanical or electrodynamical viewpoint was adopted until quite recently.

The birth of the subject of electron optics may be said to have occurred in 1926, when H. Busch (B. 13) showed that the action of a short axially symmetrical magnetic field on electron rays was similar to that of a glass lens on light rays. In 1931 and 1932, C. J. Davisson and C. J. Calbick (D. 1) and independently E. Briiche and H. Johannson (B. 7) recognised that axially symmetrical electrostatic fields could also be used as "electron lenses". The use of electron lenses for the projection of extended electron images has since been developed, first by M. Knoll, E. Ruska and their collaborators (K. 5), who worked mainly with magnetic lenses, and then by E. Briiche and his collaborators (B. 11), who worked mainly with electrostatic lenses. In recent years electron optics has experienced a rapid development, induced by a strong industrial need. Large companies which were especially interested in building up and producing a television technique of electronics employed considerable staffs of scientific workers who were engaged to an appreciable extent with fundamental research on electron optics. Thus the research laboratories of "Electric and Musical Industries" in England, of the "Radio Corporation" in U.S.A., of "Telefunken" and "A.E.G." in Germany, and of "Philips" in Holland, have played a very prominent part in the development of the electron optical science.

The fundamental theory of electron optics is based on W. R. Hamilton's conceptions of the identity of the optical description of the path of a light ray through refractive media and the mechanical description of the motion of a mass point through a potential field. These general conceptions were presented as early as 1828-1837; they originally started from a comparison of Fermat's principle of least time as applied to the path of a light ray, with Lagrange's principle of least action as applied to any mechanical movement. The conception of an electron did not then exist, and the subject of electron mechanics did not come into existence until sixty years later (J. J. Thomson, W. Kaufmann, 1897), and another thirty years more had to elapse before the development of the optics of the electron was started.

The comparison of Fermat's and Lagrange's principles shows immediately that the path of an electron through an electrostatic field with the potential function V may be identified with the path of a ray of light if the index of refraction N for the ray is chosen to be

$$N = k\sqrt{V}, \tag{1.1}$$

k being a constant.

Equation (1.1) may be.illustrated by the elementary example shown in Fig. I - I . There a beam travelling through a medium with a refractive index N passes into another medium with a refractive index N'. The angle of incidence α and the angle of refraction *ex!* are connected by Snell's law:

$$\frac{N}{N'} = \frac{\sin \alpha'}{\sin \alpha}. \tag{1-2}$$

This optical law may be interpreted mechanically in the way which Newton used to explain the refraction of light at a glass surface. Suppose an electron travelling with uniform speed u through a space of constant potential V, passes a potential step into a space with another homogeneous potential V', so that the path of the electron suddenly changes its direction. Assuming, as in Fig. 1.1, that the potential V is more positive than V, the normal velocity component of the electron u_y is increased and the

electron is accelerated. The tangential component u_x remains

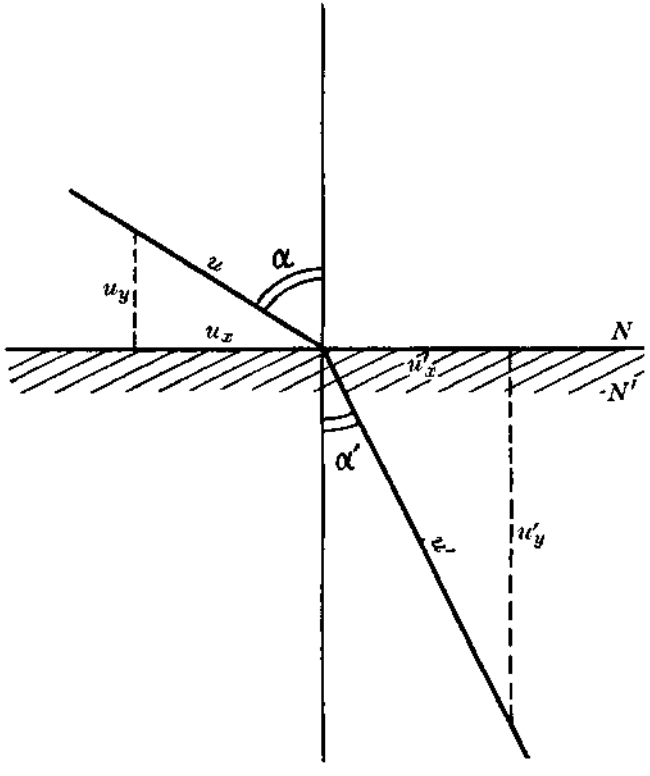

Fig. 1.1. Refraction of an electron beam.

unchanged, so that $u_x = u_x'$. Now, according to the principle of conservation of energy:

$$eV = \frac{mu^2}{2} \tag{1·3}$$

or

$$u = \sqrt{\frac{2e}{m}}\sqrt{V}, \tag{1·4}$$

where e is the charge and m is the mass of the electron. Thus the velocity of the electron is proportional to the square root of the potential. Moreover,

$$\sin\alpha = u_x/u,$$
$$\sin\alpha' = u_x'/u'.$$

Therefore

$$\frac{\sqrt{V}}{\sqrt{V'}} = \frac{\sin\alpha'}{\sin\alpha}. \tag{1.5}$$

The comparison of eq. (1.5) and eq. (1.2) leads again to the fundamental law of eq. (1.1). For convenience we may measure the refractive index $N = \sqrt{V}$ here and throughout the book by the square root of the voltage.

There should be mentioned one principal difference between the great majority of the light optical and the electron optical arrangements. The light rays are generally refracted by a finite number of refracting surfaces where the refractive index changes suddenly, whereas in electron optical arrangements the refractive index changes continuously along the path of the electron. However, this difference is not an important obstacle in the application of practical light optical methods to electron optical problems. It is always possible to divide the range of the continuously changing potential into a finite number of steps of an assumed constant potential corresponding to a finite number of different sheets of constant refractive index. It can, for instance, be shown that the path of an electron may be traced through an electrostatic electron lens by a repeated application of Snell's law. In this case a theoretical splitting up of the continuously varying field into a finite number of steps is sufficient to obtain results of high accuracy (K. 3).

The optical description of the motion of the electron in a magnetic field is not as obvious as it is in an electrostatic field. For magnetic fields there does not exist a simple scalar magnetic potential, analogous to the electrostatic potential, which can easily be elucidated by obvious analogies such as that of a little ball rolling on a curved material surface. Under the influence of the magnetic field, the electron performs a spiralling motion in space, so that an optical analogy would seem rather complicated. However, it will be pointed out in Chapter v that for all axially symmetrical arrangements the problem can generally be reduced to a two-dimensional one by tracing the movement of the electron in a meridional plane which rotates, together with the electron, round the axis of its spiralling motion. In this meridional plane, there can be defined a "meridional potential" which is easily derived from the well-known vector potential of the magnetic

field. It will be explained that the electron is refracted at the equipotentials of this meridional potential in essentially the same manner as at the equipotentials of the electrostatic field.

Discussing the electron optical problem under the most general conditions, we have to ask how the refractive index for the electron beam has to be composed if there exist electrostatic as well as magnetic fields, and whether there exist still other potentials besides the electrostatic and the meridional-magnetic one. The answer to this question may be readily derived from Maxwell's equations, from which the following integral form can be obtained (S. 3):

$$F = e\left[\frac{u}{c}\,\mathrm{curl}\,A\right] - e\frac{1}{c}\frac{\partial A}{\partial t} - e\,\mathrm{grad}\,V, \qquad (1{\cdot}6)$$

F being the total force acting on the electronic charge e; u being the velocity of the electron, A the magnetic vector potential, and V the electrostatic potential. This equation is particularly convenient for electron optical considerations, as it shows clearly the sort of potentials acting on the charge of the electron. The force F is composed of three parts, the first is generally called the electrokinetic force due to the motion of the electron in a stationary magnetic potential field, the third is the electrostatic force due to the action of the electrostatic potential, while the second is Faraday's electrotonic force due to the retardation of the potentials or to the finite velocity of propagation of the fields caused by rapidly moving charges. Since we shall here consider stationary conditions only, the electrotonic forces may be neglected in all electron optical considerations and the refractive index for the electron beam can be obtained by superposition of the electrostatic and the magnetic effects.

At this stage it may be asked whether there is any advantage in discussing the action of potentials on electrons from the optical point of view, since, at first sight, such a discussion might appear to be no more than a modern analogy for talking about the old problem. To take a simple example, there is certainly not much point in calling a homogeneous electric or magnetic deflecting

field an "electric prism", or a "magnetic prism", as is often seen in modern literature. However, in dealing with axially symmetrical fields, the merits of optical methods are evident. It need only be mentioned that in these axially symmetrical systems or "electron lenses" the path of electrons travelling close to the axis is well described by the specification of the six "cardinal" points. Thus the "collinear relationship", familiar in optics is immediately at our disposal for a relatively simple study of the action of even very complicated electric and magnetic fields on the electron.

In the following chapters we shall point out how the cardinal points can be measured and how Gaussian optics is applied to electric and to magnetic lenses. We shall also deal with the focusing of wide beams and with the projection of extended "electron pictures", and in this connection we shall have to study the main features of the errors of electron lenses. After the theoretical discussions the full benefit of the practical application of the optical principles, especially the experience of glass-optical lens design, will become available for technical purposes. We shall elucidate the principles of electron guns as used in television, of electron microscopes, and of picture transformers and other electron optical devices. The invention or the rapid development of all these modern instruments would be unthinkable without the help of the new science: Electron Optics.

Chapter II

THE CARDINAL POINTS OF AN ELECTRON LENS

A true optical image is formed if any point of the image space corresponds to a conjugate point of the object space. Straight lines, connecting two points, are in the ideal case reproduced as straight lines, and planes are reproduced as planes. Mathematically such a transformation can be obtained if the three co-ordinates of the object space are linked up with the three co-ordinates of the image space by a system of three linear equations forming a so-called collinear relationship. In the case of axially symmetrical systems the collinear relation between the two co-ordinates of each space reduces to a system of two equations containing five constants if it is confined to axially symmetrical systems. These constants define the six cardinal points of the system, namely the two focal points, the two principal points, and the two nodal points.*

The mathematical scheme of the collinear relationship cannot be fully realised in the case of an actual physical lens system, since it is to some extent in contradiction with fundamental physical laws, such as Fermat's principle of least time, or with the second law of thermodynamics. In a later chapter we shall discuss how far the peculiarities of an ideal image could be realised.

At first we will confine our considerations to paraxial rays only, that is, rays which are travelling so closely to the axis of the system, that the sine of the angle Θ between a ray and the axis given by

$$\sin \Theta = \Theta - \frac{\Theta^3}{3!} + \frac{\Theta^5}{5!} + \dots \qquad (2{\cdot}1)$$

may be put equal to Θ. In this case the terms of higher order are

* **About sign conventions, see (P. 2).**

neglected, and the approximation is called the first order theory. In this theory the collinear relationship holds sufficiently well and thus even the properties of actual physical lens systems can be described to some extent by the location of the six cardinal points. We shall start with an explanation of these points in the case of the simplest electron lens. We will also discuss how these points can be located experimentally and how the knowledge of their position can be used for practical purposes.

The simplest arrangement acting as an electron lens consists of two coaxial metal tubes which are kept at different electrostatic potentials. In Fig. 2.1 are shown two tubes of equal

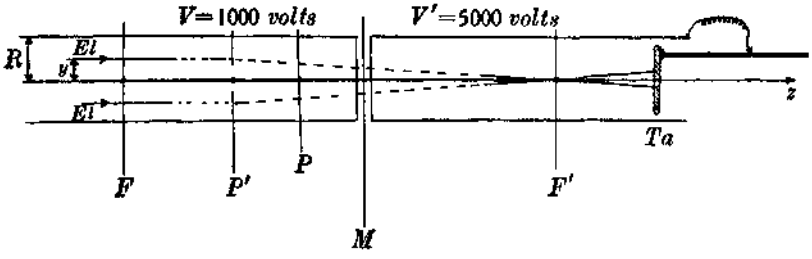

Fig. 2.1. Investigation of an electron lens by means of a sliding target.

diameter, the left one at the lower electric potential *V*, the right one at a higher potential *V*. In order to specify a concrete example, it may be assumed that V=1000 volts and V' = 5000 volts. Both tubes lie symmetrically about an ideal plane, the so-called midplane of the system, cutting the axis of rotational symmetry (the z-axis) at the point *M*. By a special arrangement, which will not be described at the moment, electron beams El, travelling exactly parallel to the z-axis, are transmitted through the tubes. These electrons are gradually accelerated from the lower potential *V* to the higher potential *V*, and in passing through the electric field they are also gradually deflected. The path of the beams can be investigated by means of a small target *Ta* which is covered with fluorescent substance. This target is kept at the potential *V* of the second tube and can be moved along the axis of the tube. All points where the electron beams hit the target are

visible by fluorescence, so that the distances of the beam from the z-axis can be everywhere determined.

To avoid disturbances of the field of the lens, the target should be kept outside the lens, i.e. in the field-free space where the electrons travel along perfectly straight lines. The path of the beams inside the lens is actually curved. The straight, broken lines drawn in Fig. 2.1 are obtained by extrapolation of the measured parts of the paths.

It will be noticed that the electron beams intersect at one point, the focus P'. Extrapolating the straight part of a traced electron beam backwards until it cuts the prolongation of the original parallel beam one finds the principal plane, which intersects the axis in the principal point P'. Assuming parallel beams starting from the high voltage side of the lens (i.e. coming from the right side of Fig. 2.1), the electrons would be decelerated and focused at a point P. The intersection of the extrapolated original parallel beam and the extrapolated final direction would show the other principal point P. Thus, by this simple experiment there can be found four cardinal points P, P' and P, F' of the electron lens. The two remaining ones are the nodal points K and K'. They lie in the same direction as the principal points with reference to the respective focal points, but are shifted by the difference between the numerical values of the two focal lengths, thus

$$\left.\begin{aligned} KF &= PF + |P'F' - PF| = P'F' \\ K'F' &= PF \end{aligned}\right\}. \qquad (2.2)$$

Therefore if the focal points and the principal points are obtained experimentally, the nodal points can be located by an easy procedure. For a general estimate of the position of the cardinal points it may be helpful to notice that for all two-electrode lenses, both principal points lie on the same side of the midplane; they also lie at the low voltage side where the refractive index is small. The principal points as well as the nodal points are crossed over with respect to their appropriate focal points.

The location of the cardinal points for any axially symmetrical electric field is of the greatest practical importance. Their position

controls the size and position of the electron image of any source of electron rays. This may be explained by Fig. 2.2. There, F and F' are the two focal points and P and P' the two principal points, IB the electron source. At I' there can be detected (for instance by means of the sliding fluorescent target) a sharp electron image. In the example of Fig. 2.2 this image $I'B'$ is found to be slightly demagnified in comparison with the object IB. By the following simple construction this image can be found graphically. A beam,

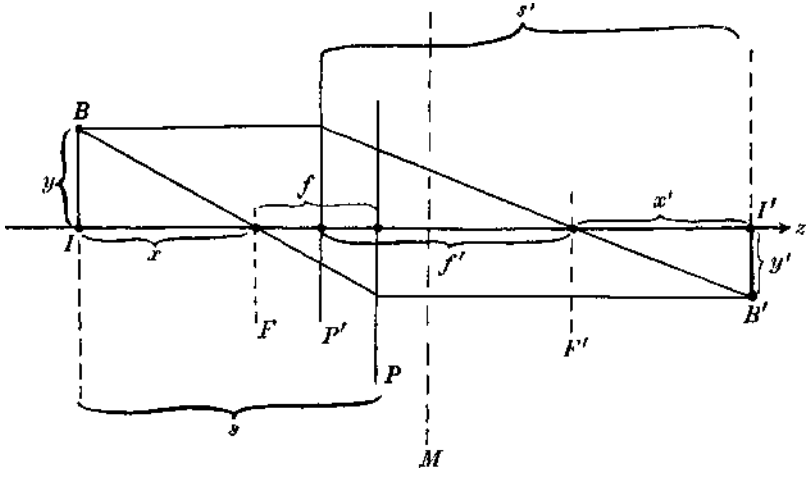

Fig. 2.2. Location of an optical image. Lateral magnification.

parallel to the z-axis drawn through a point B of the object, is refracted at the principal plane through P' so as to pass through the focus F'. Another beam emerging from B and travelling through the focus F is refracted at the principal plane through P and leaves the lens in a direction parallel to the axis. The two rays intersect at B', where the image is formed. Taking $IF=x$ and $I'F' = x'$ as object and image distances, measured from the foci, and taking FP=/and $F'P'=f$ as the focal lengths of the system and $IB=y$ and $I'B' =y'$ as object and image size, it can be seen from Fig. 2.2 that the following relation holds for the lateral magnification y'/y:

from which Newton's formula

$$XX' = ff \tag{2.4}$$

is derived. Moreover, taking $s = f + x$ and $s' = f' + x'$ as the object and image distances from the appropriate principal points, there follows from eq. (2.4):

$$(s - f)(s' - f') = ff'$$

or

$$\frac{f}{s} + \frac{f'}{s'} = 1. \tag{2·5}$$

The angular magnification or ratio of conjugate divergences is defined as the ratio of the two angles which two conjugate beams

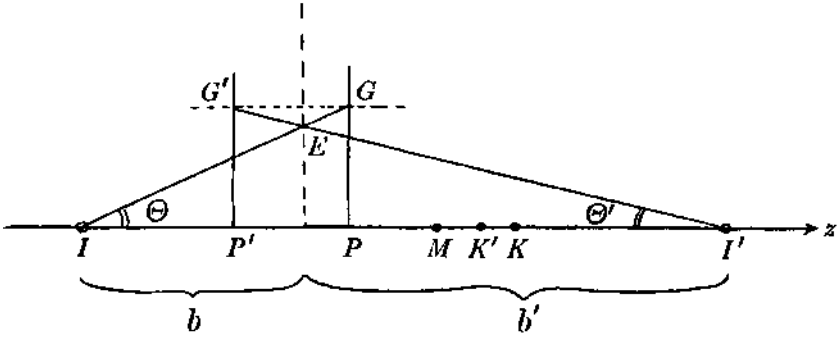

Fig. 2.3. Divergence of a beam. Angular magnification. Thin equivalent lens.

make with the axis. The angles maybe so small that their tangents are substantially equal to their radian measure. In Fig. 2.3 object and image points are represented by I and I', and the two conjugated divergences are Θ and Θ′.

From Fig. 2.3 one reads immediately

$$\frac{\Theta}{\Theta'} = \frac{IP}{I'P'} = \frac{s}{s'} = \frac{f + x}{f' + x'},$$

and using eq. (2·4)

$$= \frac{f + x}{f' + \dfrac{ff'}{x}} = \frac{(f + x)\,x}{f'(x + f)} = \frac{x}{f'}. \tag{2·6}$$

The angular magnification Θ/Θ', and the lateral magnification y/y' are connected by one of the most important relations of the first order theory. This is Lagrange's law:

$$N\Theta y = N'\Theta' y'. \tag{2.7}$$

When the refractive index is replaced by the square root of the electrostatic potential (see Chapter i) one obtains

$$\sqrt{V}\Theta y = \sqrt{V'}\Theta' y'. \tag{2.8}$$

In glass optical textbooks, Lagrange's law is generally derived by considering the refraction of a paraxial beam at a series of spherical surfaces according to Snell's law. However, it follows for paraxial rays from quite general laws such as Fermat's principle or the thermodynamical principles and thus it may be presented here as a fundamental postulate and a special proof may be avoided.

Combining Lagrange's principle eq. (2.8) with the first and the last item of eq. (2·6) and replacing there x by $\frac{y}{y'}f$ from eq. (2·3) one obtains:

$$\frac{f}{f'} = \sqrt{\frac{V}{V'}}. \tag{2·9}$$

The ratio of the two focal lengths of the electron lens is equal to the square root of the ratio of the voltages at the electrodes.

The principal planes are defined as planes of unit lateral magnification, i.e. a ray arriving at one of the principal planes at a given distance from the axis will leave the other principal plane at the same axial distance. Nodal planes, that is, planes perpendicular to the axis through the nodal points, are correspondingly defined as planes of unit angular magnification, i.e. a ray passing one of these planes at an angle Θ to the axis, passes the other nodal plane with the same inclination $\Theta' = \Theta$. Thus from Lagrange's law it follows for the lateral magnification in the nodal planes $\frac{y'}{y} = \frac{N}{N'}$, or combining this result with eq. (2·3) and eq. (2.9) the expression (2.2) for locating the nodal points

is proved. Since the angular magnification in the nodal points is unity, $\tan \Theta = \tan \Theta$ or

$$\frac{y'}{K'I'} = \frac{y}{KI},$$

hence the lateral magnification is equal to the ratio of the nodal distances for any conjugate object and image.

After these theoretical considerations there may be pointed out a second experimental method for locating the cardinal points. Its application to electron optics has been described by D. W. Epstein (E. 1). Lateral magnifications have to be measured at two different object and image distances. A wire mesh "illuminated" with electrons may be used as a suitable object; suppose it is a distance p from the midplane. The image can be found by means of the sliding fluorescent target; let it be distant q from the midplane. Using again the same nomenclature as above, we obtain:

$$\left.\begin{aligned} p = IM = x + MF = \frac{y}{y'} f + MF \\ q = I'M = x' + MF' = \frac{y'f'}{y} + MF' \end{aligned}\right\}. \qquad (2{\cdot}11)$$

If p_1, q_1 and y_1, y_1' correspond to one position of the object, p_2, q_2 and y_2, y_2 to another position of the object, it follows that

$$f = \frac{p_1 - p_2}{\frac{y_1}{y_1'} - \frac{y_2}{y_2'}}, \qquad (2{\cdot}12)$$

$$MF = p_1 \frac{y_1'}{y_1} - p_2 \frac{y_2'}{y_2} \Big/ \frac{y_1'}{y_1} - \frac{y_2'}{y_2}. \qquad (2{\cdot}13)$$

The conjugate values of f' and MF' are obtained if in eqs. (2.12) and (2.13) the experimental values of p, y and y' are interchanged with those of q, y' and y.

This method of measuring the cardinal points is much more rapid than the elaborate experimental ray-tracing method which was described at the beginning of this chapter. Since, however,

the image has to be measured with paraxial rays only, the depth of focus is very large and therefore the accuracy of locating the image and of measuring the distance q is not too good.

It may be useful therefore to point out that this method might easily be modified by introducing from Lagrange's law (2.8) the angular magnifications instead of the lateral ones (K. 3). In eqs. (2.12) and (2.13), therefore, every ratio of y/y' has to be replaced by $\frac{\Theta'}{\Theta}\sqrt{\frac{V'}{V}}$. The required pairs of values of p, q, Θ, and $0'$ are found experimentally by tracing divergent pencils emitted from a point-source object and focused to a point image.

Electron lenses are generally "thick" lenses since the field produced by the one electrode penetrates appreciably into the other electrode, so that the region of varying refractive index extends over a distance which is considerable in comparison with the focal length of the lens. However, for many practical considerations it is a useful fact that there can always be found a "thin equivalent lens", i.e. an infinitely thin lens that will produce an image of the same size and in the same place as the image produced by the thick lens. For the right definition of this thin equivalent lens, the refractive indices have to be considered (H. 6) in order to obtain the right magnifications from object and image distances b and b' from this thin lens:

$$\frac{y'}{y} = \frac{b'}{b}\sqrt{\frac{V}{V'}}. \qquad (2{\cdot}14)$$

The position of the thin equivalent lens E is indicated in Fig. 2.3. It may be noticed, however, that this position is not fixed, but changes with the position of the object and image. The thin equivalent lens always lies between the two principal planes P and P', it moves gradually from P' to P, as the object I moves gradually from an infinite distance to the focus F (corresponding to a movement of the image I' from the focus F' to infinity). If the object I and the image I' are connected by straight lines with any point E of the thin equivalent lens

(see Fig. 2-3) the ratio of the object and image distances gives the right angular magnification:

$$\frac{\Theta}{\Theta'} = \frac{b'}{b}. \tag{2.15}$$

This can be seen by introducing Lagrange's eq. (2.8) in eq. (2.14). Combining eq. (2.6) with (2.15) one obtains as an expression for locating the thin equivalent lens

$$\frac{b}{b'} = \frac{s}{s'}. \tag{2.16}$$

The position of the thin equivalent lens divides the object-image distance *IF* in the ratio *IP/I'P'*, which is given by the distances of object and image from their appropriate principal planes.

Chapter III

FIELD PLOTTING AND RAY TRACING

The equipotentials are the refracting surfaces of electrostatic electron optics. They correspond to the concrete refracting surfaces of the glass lenses in ordinary optics. The electric field E is given in terms of the potential V by the general relation

$$E = -\operatorname{grad} V, \tag{3.1}$$

and the direction of the field is always perpendicular to the equipotentials.

The potential distribution in the space is completely defined by the geometry and the potentials of the electrodes. Neglecting space charges, the potential distribution can be completely calculated from Laplace's differential equation

$$\Delta V = 0. \tag{3.2}$$

But, although this theoretical possibility is very interesting in principle, an integration of eq. (3.2) under the proper conditions as given by geometry and potentials of the electrodes is generally very complicated. In the majority of practically important cases other methods have to be used.

To investigate potential distributions the experimental "method of the electrolytic trough" is of greatest practical value. This method had been used to investigate general electrostatic problems a long time before any electron optical research was started. It is based on the perfect physical analogy between the propagation of electric currents through electrolytes and the spreading of the lines of force through an electrostatic field. The general features of the method are shown by Fig. 3.1. G represents a large box or glass trough which is filled up to a level L with a weakly conducting liquid, for instance, with a solution of copper sulphate in water (about 10 mg./litre). T and T' represent the two electrodes of the lens; they are tubes cut in half

along the axis and fixed in such a way that the axis of the lens coincides with the surface of the liquid. Two large variable resistances *A* and *B* (~10,0000;) are connected to the electrodes, with a source of current *S* and with the current-detecting device *D*. The circuit is that of a Wheatstone bridge. The tip of the small probe *C* dips into the surface of the liquid. To avoid electrolysis, the source *S* should supply alternating current. A valve-oscillator of 500-1000 cycles/sec. is very convenient.

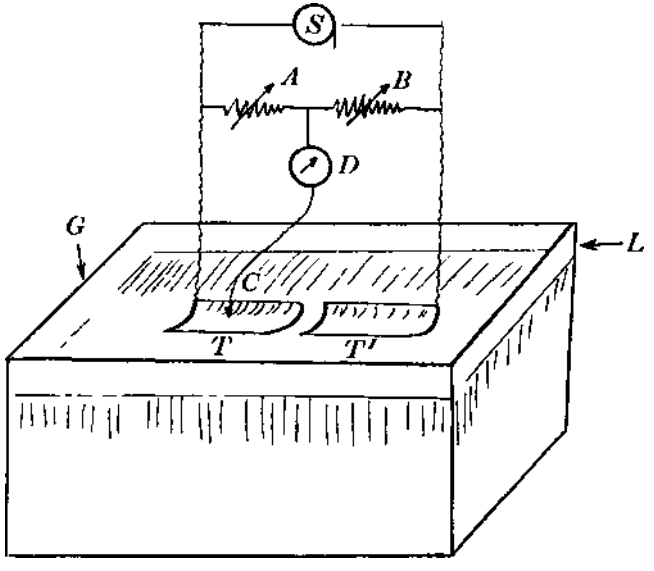

Fig. 3.1. Method of the electrolytic trough.

Headphones are suitable for the detecting device Z). For highly accurate field plotting a phase-selecting balance detector such as that described by Cosens (C. 3) may be used, in order to avoid disturbances due to a shift of the phase angle by the capacity of the electrodes. The detecting device *D* should indicate no current as soon as the probe is in the equipotential line corresponding to the adjustment of the ratio of the resistances *A* and *B*.

The potential of the probe may be marked as a percentage of the total potential difference between the two electrodes. For instance, if *A* = *B*, the probe is at the 50% equipotential, or if

$A\backslash B = 1/9$, the probe is at the 10 % equipotential, etc. In this way one obtains a very general diagram, and the potential plot can easily be interpreted for all varieties of voltages or voltage ratios at the electrodes, since it is evident that the shape of the equipotentials does not change if the voltage at either of the two electrodes is altered. For instance, the two tubes may have the potentials V=1000 volts and V'= 5000 volts. In this case the 10% equipotential would be at

$$1000 + \frac{10}{100}(5000 - 1000) = 1400 \text{ volts.}$$

In another example, the same two tubes may be at V=500 volts and $V = 20{,}000$ volts; then the 10% equipotential would be at 2450 volts. The 1400 volt equipotential of the first example would be in exactly the same place as the 2450 volt equipotential of the second example.

An appreciable simplification of the field-plotting arrangement for the particular case of rotational symmetrical fields has been proposed by M. B. Manifold and F. H. Nicoll (M. 2) and the new method has been used successfully for some time in the E.M.I. Research Laboratories. The new method is based on the fact that it is permissible in problems of conduction to introduce an insulating barrier along any surface across which there is no flow of current. Thus the system can be cut by two diametrical planes producing a wedge. Such a wedge is realised in practice by a tilted trough containing electrolyte, resting on a plane, insulating bottom. If the angle of the wedge is small, the electrodes used in it need not be surfaces of revolution but can be replaced by pieces of metal sheet bent to the shape of a longitudinal section of the actual electrode. For instance a two-tube lens is simply represented by two flat strips of metal placed in the liquid in a direction parallel to the thin end (= tube axis) of the wedge.

In Fig. 3-2 there is shown an actual potential plot of the symmetrical two-tube lens. Equipotentials are plotted in steps of 10% between 10 and 90%, and to show the spreading of the

field into the tubes, extra equipotentials are plotted at 2.5,5, 95 and 97.5%. One can see that the whole figure is perfectly symmetrical with respect to the midplane. Moreover, the potential gradient is greatest at the midplane, where the equipotentials are closest together, and it decays slowly towards the outer ends of the tubes, the 90% equipotential being distant about one tube radius from the midplane and the 97.5 % equipotential being twice as far from that plane.

It is advisable to measure every geometrical distance in terms of the tube radius R as a unit, so that it is easy to transfer the results of a field plot to electron lenses of any size. In order to

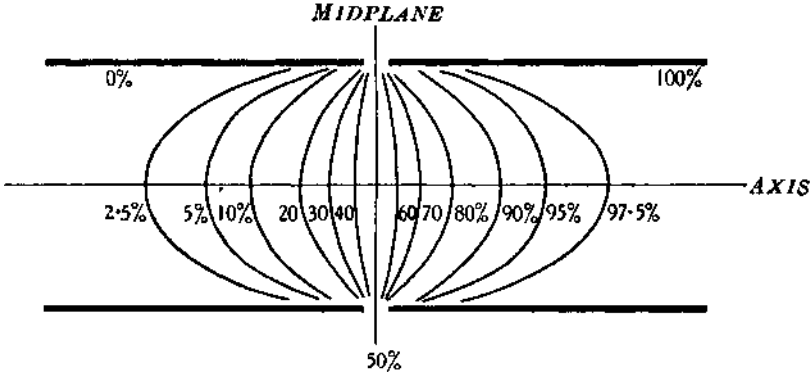

Fig. 3.2. Potential distribution in the symmetrical two-tube lens.

obtain good accuracy in plotting the equipotentials, the model of the electrodes should be made as large as the size of the trough allows. Other metal parts and insulators should, however, be sufficiently removed in order to avoid disturbances. Insulators, such as the glass wall of the trough or the surface of the liquid containing the axis of the electrode arrangement, act like mirrors towards the equipotentials. In this way it is possible to use the halves or even small sectors of the electrodes only, as any plane through the axis is also a plane of symmetry in the axial symmetrical arrangement. On the other hand, conductor surfaces are equipotentials. If, for example, in order to avoid external disturbances, the ends of the tubes in the electrolytic trough are

closed by metal sheets, kept at the tube potential, these sheets must be sufficiently far away from the midplane in order to avoid any influence on the equipotentials to be investigated. According to practical experience, a plane sheet perpendicular to the axis and distant three tube radii from the midplane would not modify markedly the shape or position of the 95 % equipotential.

When a part of the whole potential plot has to be investigated with increased accuracy, metal sheets could be shaped exactly like a natural equipotential measured in the electrolytic trough, and could be introduced in the trough. For example, the midplane was found to coincide exactly with the 50% equipotential. Therefore, a plane metal sheet connected to the end of the resistance *A* may be used instead of the tube *T* in Fig. 3-1. The probe would then measure the same equipotentials in the tube T" as given in Fig. 3.2, only the designation of the equipotential would no longer be given by the ratio *AjB* of the resistances but in the present example by (50 + A/2B)%. Generally, two metal sheets replacing the equipotentials of *n* and *m%* may be connected to the ends of the resistances *A* and *B*. The right designation of any measured equipotential is then given by

$$n+\frac{m-n}{100}\frac{A}{B}. \qquad (3.3)$$

By this artifice of replacing two equipotentials by metal sheets a relatively small fraction of the whole field could be investigated separately on a scale enlarged as much as the dimensions of the electrolytic trough would allow, and plots of considerable accuracy could be obtained, even with small troughs.

After having obtained an exact potential plot of the investigated electron lens with all the values of the equipotentials calculated in volts, the path of any electron could be traced in principle by an immediate application of Snell's law. The spaces between the equipotentials V_1 and V_2, V_2 and V_{s3}, V_3 and F_4, etc. are assumed to be media of constant refractive indices $N_1 = V_1$, $N_2 = V_2$, $N_3 = V_3$, etc. Using a protractor of high accuracy, the angles of refraction a_1', a_2', a_3', ... as calculated by means of

eq. (1-5) of Chapter 1 from the angles of incidence α_1 α_2, α_3, ... may be plotted, the path of the electron between two equipotentials being drawn as a short straight line. However, such a procedure turns out to be of little value. It is very inaccurate, due to the difficulty in finding the exact direction of the normals to the equipotentials which are needed to plot the angles a and a'.

Much more helpful is the method of trigonometrical ray tracing being quite commonly used in glass optics. It is based on the following four computing formulae, which are quite old and probably date back to the eighteenth century:

$$\sin \alpha = \sin \Theta \frac{(l+r)}{r}, \tag{3.4}$$

$$N' \sin \alpha' = N \sin \alpha, \tag{3.5}$$

$$\Theta' = \alpha' - \alpha + \Theta, \tag{3.6}$$

$$l' = r \frac{\sin \alpha'}{\sin \Theta'} - r. \tag{3.7}$$

To elucidate these formulae, we might explain that in ray tracing the initial data available are (see Fig. 3.3)

Θ = the angle between the initial beam and the axis,

/ = the distance from the refracting surface of the intersection of initial beam and axis,

r = the radius of curvature of the refracting surface which is assumed to be of spherical shape, and

N/Nl' = the ratio of refractive indices at both sides of the refracting surface.

Eq. (3.4) is obvious from inspection of Fig. 3.3. It enables sin a to be calculated, and then from eq. (3.5) (Snell's law) sin a' is obtained. From eq. (3-6) which is again obvious from Fig. 3-3, there is calculated $0\backslash$ the angle of the refracted ray. From eq. (37) it is then possible to calculate the distance l' from the refracting surface to the point of intersection of the refracted beam and the axis. Eq. (37) can again be derived from

Fig. 3.3, or may be obtained from eq. (3.4) by interchanging dashed and undashed symbols. If the ray has to be traced through two refracting surfaces, then Θ_1 and l_1' of the first surface are equal to Θ_2 and l_2 of the second surface, but for the ratio N_2/N_2 (where $N_2=N_1'$), the index N_2 has to be given and the radius of curvature r_2 has to be given as well. Numerical examples to explain the use of trigonometrical ray tracing in glass optics can be found in the literature, and the books by Hardy and Perrin (H. 1), p. 38, or by Conrady (C. 2), p. 17 and p. 51, may be referred to.

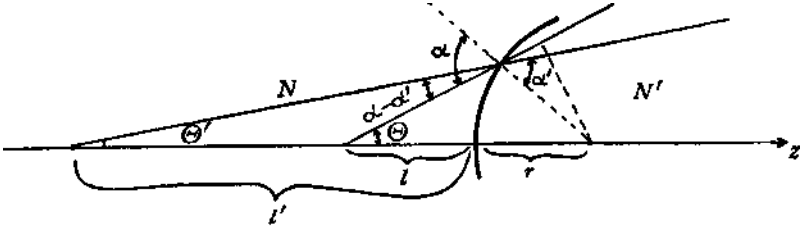

Fig. 3·3. Refraction at spherical surface.

The application of the ray-tracing method to electrostatic lenses has been described by O. Klemperer and W. D. Wright (K. 3). In their method, the continuously varying electric field of the lens is assumed to be subdivided into a finite number $n + 1$ of uniform fields bounded by n equipotential surfaces. A lens modified in this way will differ from the actual electron lens, but the difference will decrease as n increases. On the other hand, the amount of work involved in the ray-tracing procedure makes it advisable to keep the value of n as small as the request for accuracy allows. In practice it has been found convenient to subdivide an electron lens into about 10 or 20 steps of equal refraction. If N and N' are the refractive indices at the two sides of an equipotential surface, N_1 being the initial refractive index and N_n' the final refractive index, then the ratio N/N' for each surface is given by

$$\frac{N}{N'}=\sqrt[n+1]{\frac{N_1}{N_n'}}=\sqrt[n+1]{\left(\frac{V_1}{V_n'}\right)^{\frac{1}{2}}}, \qquad (3\cdot8)$$

since N is proportional to the square root of the voltage V. The required subdivision of the potentials can be obtained practically by plotting log V against the axis co-ordinate and by subdividing log V into the adopted number of equidistant steps.

Although the computing formulae (3.4)-(3"7) apply only to spherical surfaces, it is noticed at once by inspection of Fig. 3.2 that the equipotentials are generally not spherical. In that case, the compromise of using only the central portions of the equipotentials as spherical to a first order of accuracy has proved to be successful. The radii of the central portions of the equipotentials can be measured with the help of a series of templates which are fitted to the experimentally determined surfaces. From a curve of these radii against the axis co-ordinate the radii at the required points can be interpolated and the computing formulae can be readily applied. The results of trigonometrical ray tracing are of high accuracy and agree within a few per cent with the experimental data obtained from direct measurements with electron beams.

Although other theoretical methods for obtaining information about the properties of electron lenses may be less accurate, they will be shortly explained here in so far as they are either of theoretical interest or of practical value.

Instead of using graphical methods the focal length of the lens can be calculated from the data of the field plot according to a procedure introduced by J. Picht (P. 1). The electron lens is thought to be divided up into a great number of small lenses, each being formed by the sheet between two equipotentials. The focal length ${}_sf$ of such a sheet is calculated from

$$\frac{y}{{}_sf} = \tan(\alpha - \alpha') \approx \alpha - \alpha', \qquad (3{\cdot}9)$$

if a paraxial beam travelling parallel to the axis with a semi-aperture y meets the spherical surface at an angle of incidence a and is refracted at an angle a'. If r is the radius of curvature of the refracting surface and AN is the increase of refractive index N in crossing the surface, one obtains for Snell's law (3.5)

$\frac{\alpha'}{\alpha}=\frac{N-\Delta N}{N}$ and $\alpha=\frac{y}{r}$. Introducing these relations into eq. (3·9) one obtains

$$\frac{1}{{}_sf}=\frac{\Delta N}{Nr}. \qquad (3\cdot10)$$

The power of the whole lens is obtained by summing up over an infinite number of infinitely small sheets:

$$\frac{1}{f}=\Sigma\frac{1}{{}_sf}=\frac{1}{N_n}\int_{N_1}^{N_n}\frac{dN}{r}=\frac{1}{N_n}\int_{z_1}^{z_n}\frac{1}{r}\frac{dN}{dz}dz, \qquad (3\cdot11)$$

z being the coordinate along the axis. Introducing the potentials V,

$$\frac{1}{f}=\frac{1}{\sqrt{V_2}}\int_{z_1}^{z_2}\frac{1}{r}\frac{d\sqrt{V}}{dz}dz. \qquad (3\cdot12)$$

This relation can be further developed by eliminating r. From Laplace's law (3.2) it is possible to deduce that the radius of curvature of the equipotentials at the axis is proportional to the ratio of the two derivatives of the potential along the axis

$$r=2\frac{dV}{dz}\Big/\frac{d^2V}{dz^2}. \qquad (3.3)$$

It is of principal importance that the properties of an electron lens for paraxial rays can be calculated if only the potential distribution along the axis is known (J. 2). A formula like eq. (3.12) is, however, of limited value, because it implies that the potential along the axis is expressed by an analytical function. Moreover, this formula represents only a first approximation, since a summation such as that of eq. (3.11) applies strictly for very thin lenses only, and from field plotting data it is known that all electron lenses extend over a considerable space.

In this connection it is therefore of some interest that I. G. Maloff and D. W. Epstein (M. 1), starting from electron mechanical considerations, developed a graphical method to find the paraxial electron path from the axial potential distribution. The method produces rather accurate results, but it is complicated in use and cannot be described here in detail.

Of greatest practical importance for electron ray tracing are

the automatic tracing machines which have been developed by D. Gabor (G. i) and D. B. Langmuir (L. i). Although these machines are complicated devices which could not quickly be produced by everybody, the underlying principle is of sufficient interest to be explained here shortly. A probe dipping into an electrolytic trough is rigidly connected to a small carriage which guides a pencil drawing the electron path. The carriage is automatically steered by an electric motor. The steering angle is adjusted in the following way. The probe is split up into two wires arranged so that the line joining them is perpendicular to the electron path. Thus it measures not only the potential difference V of the particular point relative to the origin of the electron (for instance the cathode), but also the potential gradient V_n in the direction normal to the trajectory. Now the centrifugal force acting on the electron is given by

$$eV_n = \frac{mu^2}{\rho}, \tag{3.14}$$

where p is the radius of curvature of the path, and u the linear velocity of the electron. If the energy equation is written in the form

$$eV = \frac{mu^2}{2}, \tag{3.15}$$

p is then given by

$$\rho = \frac{2V}{V_n}. \tag{3.16}$$

Thus the steering angle (= 2a), i.e. the angle included by the two axles of the carriage, has to be adjusted at each point in order to produce the path with the radius of curvature p as given by eq. (3*16). As can be seen in Fig. 3-4, this path will be followed, if the two planes which are defined by the rims of the wheels, W_1 W_2 and W_3, are kept parallel to the tangents of the path. In this case, the loci for the centre C of the circle with the radius p are: (1) the prolongation of the axle of the wheels W_1 and W_2 which is rigidly connected with the carriage, and (2) the bisecting line of the angle between the planes parallel to

the wheels which passes through the pivot of the wheel W_s which is steered. Under these conditions it follows immediately

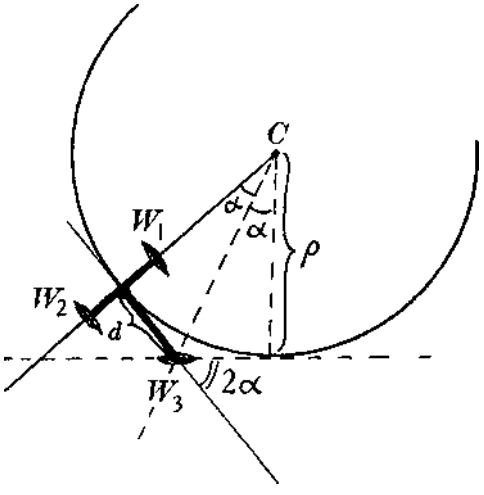

Fig. 3.4. Automatic ray-tracing apparatus.

that $\cot \alpha = p/d$ if d is the distance between the pivot and the fixed axle. The small motor, which automatically steers the carriage, can therefore conveniently be operated by an electric bridge circuit controlled by the two voltages V and V_n.

Chapter IV

SOME ELECTROSTATIC ELECTRON LENSES

From the considerations of Chapter III, it becomes obvious that all properties of an electrostatic electron lens are defined by voltage ratios, the absolute value of the potentials at the electrodes being unimportant. The voltage ratio* alone defines the position of the cardinal points. For instance, in eq. (3.8) the ratio of refractive indices which is responsible for the angle of refraction at each equipotential is given by *VJVJj* so that, for example, the cardinal points which have been drawn in Fig. 2.2 would be in exactly the same position whether the potentials at the two tubes were 0.1 and 0.5 volt or 10 and 50 kilovolts respectively. With electrostatic lenses, it is convenient to measure all geometrical lengths in terms of the radius of one of the electrodes. For instance, the symmetrical two-tube lens of Fig. 2-i with the voltage ratio $V'/V = 5$ has the two midfocal lengths: $MF = 5.15R$ and $MF' = 4.4R$. Thus if the radius of the tube were 2 cm., these midfocal lengths would be 10.3 and 8.8 cm. respectively, or with tubes of twice this radius, the midfocal lengths would be twice as large.

The positions of the focal points depend very much on the voltage ratio. In Fig. 4.1 there are plotted the two midfocal lengths of the symmetrical two-tube lens measured in tube radii, as a function of the voltage ratio. The curve denoted by D.P. belongs to the focus, which is obtained when parallel electron rays are decelerated, it corresponds to *MF* in Fig. 2.2. The other curve A.P. gives the midfocal lengths corresponding to *MF'* in Fig. 2.2, *F'* being the focus obtained when parallel beams are accelerated by this lens. The distances of the two

*** In the literature, the voltage ratio is often called "focusing ratio*'.**

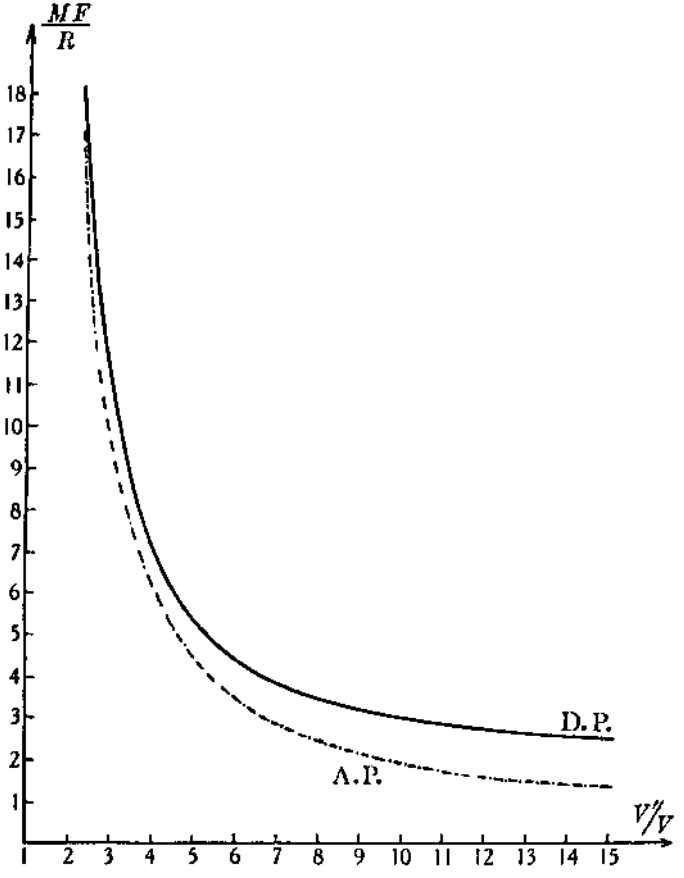

Fig. 4·1. Midfocal length of the symmetrical two-tube lens.

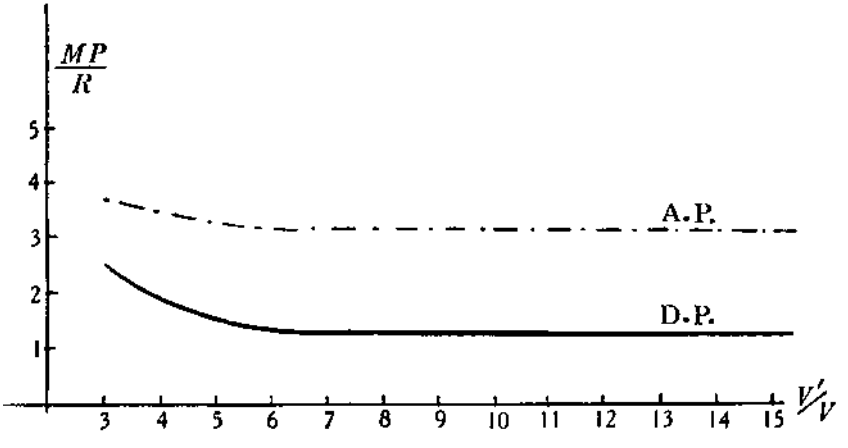

Fig. 4.2. Position of principal planes of the symmetrical two-tube lens.

corresponding principal planes from the midplane, as a function of the voltage ratio, are shown in Fig. 4-2, the curve D.P. corresponding to the principal plane *P* in Fig. 2-2, and the curve A.P. corresponding to P\ The position of the principal planes changes very little with the voltage ratio. Both midfocal lengths, however, decrease rapidly with increasing voltage ratio. For instance, at a voltage ratio 2 both midfocal lengths are of the order of 20 tube radii, and at a voltage ratio of 15, they are both of the order of 2 tube radii. In all cases, and especially for high voltage ratios, the "A.P.-midfocal length" is shorter than the "D.p.-midfocal length".

Since the two-tube lens always makes the electron beam more convergent it is a positive lens, and this is true whether it accelerates or decelerates the electrons. Ray-tracing results show that the two-tube lens can be considered as consisting of two "semilenses", a positive one having equipotentials convex towards the lower potential side and a negative one, making the beam more divergent, having the equipotentials concave towards the lower potential side. As can be seen from Fig. 3.2, the midplane separates the two semilenses. The power of the positive semilens is always greater than that of the negative semilens, so that its effect predominates in the resulting full lens. In Fig. 4-36, there are shown the paths of the two characteristic parallel beams D.P. and A.P. The glass-optical analogies of the semilenses are also shown in Fig. 4.3 *a* as convex and concave lenses. The voltage ratios of the semilenses could be defined as the voltage ratio between the midplane and the first of the tubes, and as the voltage ratio between the other tube and the midplane. The values of these voltage ratios are

$$\left(\frac{V'-V}{2}+V\right)\Big/ V=\frac{V'+V}{2V} \qquad (4\cdot1)$$

for the positive semilens, and

$$\frac{2V'}{V'+V} \qquad (4\cdot2)$$

for the negative one. Thus the voltage ratio of the positive semilens increases without limit as a linear function of the total voltage ratio *V'/V*, but the voltage ratio of the negative semilens, being always smaller than that of the positive one, approaches the value 2 as an upper limit as the total voltage ratio is increased indefinitely. If the electrons were accelerated and sufficiently high voltage ratios were applied, the electrons might cross over very close to the midplane, and any beam would leave the lens more divergent than it entered. If the voltage ratios were still higher, for instance of the order of 1000, it could happen that the beam crossed over early in the first semilens and left the lens converging, thus crossing over finally a second time.

The positions of the nodal points of the electron lens, which are important for a discussion of the magnification, can be calculated from the data of Fig. 4.1 and Fig. 4.2 by means of eq. (2.2). In this way it is found that both the nodal points usually lie on the high voltage side of the midplane and are crossed over with respect to their corresponding focal points. The position of the nodal points changes but slightly with the voltage ratio.

The fact that the two nodal points are on the high voltage side suggests that the magnification *y'\y* of an image *y'* produced on the high voltage side would be smaller than a magnification calculated as the ratio *qjp* of mid-image to mid-object distance. As these two distances are always easy to measure, it is of some practical interest to know the order of magnitude of a factor *g* which indicates how much smaller the actual magnification is than the ratio of *q* and p. Using eqs. (2.3) and (2.11) one calculates:

$$g=\frac{p\,y'}{q\,y}=\frac{(x+MF)}{(x'+MF')}\frac{f}{x}=\frac{x+MF}{f'+\dfrac{xMF'}{f}}=\frac{x+MF}{MF'+MP'+\dfrac{xMF'}{MF-MP}}. \tag{4·3}$$

By substituting practical values for /, /', *MF* and *MF'* (dashed indices represent high voltage side), it can be recognised that *g*

lies generally round 70 %, tending to slightly smaller values when either the voltage ratio or the object distance is decreased.

The approximate constancy of g involves the following curious result. If the values of p and q are given, an image can be obtained by using either large or small tubes. If large tubes are used the voltage ratio has to be relatively higher, but the mid-object distance as measured in tube radii (p/R) becomes relatively smaller. The surprising result appears, however, that for a given p and q the magnification can scarcely be varied by

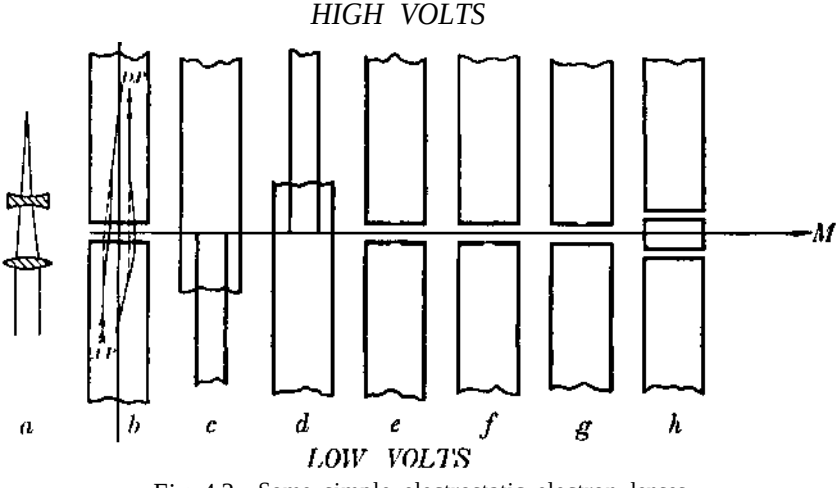

Fig. 4.3. Some simple electrostatic electron lenses.

changing the size of the tubes, although this change may include very large corresponding changes of the ratio of refractive indices of object and image space.

The position of the cardinal points, and therefore the value of the magnification for a given object and image position, can be slightly varied if the shape of the electrodes of the electron lens is changed. There exists a very large variety of shapes and we have to confine ourselves to mentioning just a few simple types in order to explain the principal characteristics and possibilities. In Fig. 4.3 b-g are shown six examples of two electrode lenses produced by combinations of cylindrical tubes and straight diaphragms. The straight line M, drawn through all the lenses, coincides in each case with the midplane. Only in

lenses *b* and *e* does the midplane represent a plane of symmetry; in the other cases it is a rather arbitrary plane of reference. As a unit of length, it is practical to take the radius *R* of the largest electrode, since this radius is limited by the size of the evacuated glass tube containing the electron lens. In Table 4/1 are given the data concerning midfocal lengths *MF* and *MF'* and the distances *MP* and *MP'* between the principal points and the midpoint, the plain symbols corresponding to the decelerated parallel beam D.P., the dashed ones to the accelerated parallel beam A.P. In the last column references are given to papers which deal with the corresponding types of lenses. It can be seen that the given values are markedly different, although the voltage ratio was taken as the same *(V'/V=5)* in all cases. In order to understand the results, we may consider again that any one of these electron lenses can be thought of as consisting of two semilenses which are separated by the midplane. A large decrease in focal length would then be expected if the smaller electrode is on the low voltage side. The smaller electrode

TABLE 4.1

Experimental data concerning the location of foci F and F' and principal points P and P'

Fig. 4·3	Electrodes, radius		5 D.P. *MF*	5 A.P. *MF'*	5 D.P. *MP*	5 A.P. *MP'*	Potential at *M*	Literature
	At low volts	At high volts						
b	Tube, *R*	Tube, *R*	5·4	4·4	1·4	3·1	50 %	K. 3
c	Tube, *R*/2	Tube, *R*	2·6	3·2	0·1	1·0	31 %	E. 1
d	Tube, *R*	Tube, *R*/2	4·3	3·4	1·5	2·3	69 %	E. 1
e	Diaphragm, *R*/4	Diaphragm, *R*/4	1·5	1·4	0·4	0·9	50 %	B. 1, H. 6
f	Diaphragm, *R*/4	Tube, *R*	2·4	2·9	1·3	0·5	13 %	—
g	Tube, *R*	Diaphragm, *R*/4	4·4	3·2	1·9	2·6	87 %	—

would then correspond to the positive semilens (Fig. 4.3 *a),* which always overpowers the negative semilens, as was pointed out at the beginning of this chapter. The results obtained with lenses 4.3 c and 4.3f support this expectation qualitatively, although the decrease in focal length is rather less than pro-

portional to the decrease in electrode radius. Moreover, if the smaller electrode is at the high voltage side, it corresponds to a negative semilens, which, according to the above considerations, should not greatly affect the focal length of the complete lens. The results show, however, that even here the focal length of the complete lens is appreciably decreased in comparison with the symmetrical two-tube lens. The reason for this reduction of focal length with diminishing dimensions of the high voltage electrode becomes obvious when a field plot of an unsymmetrical arrangement* is inspected. The midplane then no longer coincides with any equipotential. The 50 % equipotential has become concave towards the smaller electrode and has penetrated appreciably into the larger electrode. The axial co-ordinate at which the curvature of the equipotentials changes its sign is generally not far away from the midpoint. The potential at the midpoint is more removed from 50 % the greater the difference between the sizes of the two electrodes. In column 8 of Table 4-1 are noted the actual potential values at the midpoint of the lens. It can be seen that in all cases the voltage ratio of the semilens in the smaller tube is decreased and the voltage ratio of the semilens in the larger tube is correspondingly increased with respect to the voltage ratios of the semilenses in the symmetrical two-tube lens (eqs. 4.1 and 4.2). Thus if the dimensions of the electrode at the high voltage side are reduced, the decrease of focal length and the shifting of the principal points of the complete lens can be understood to be caused by increasing voltage ratio of the positive semilens which is contained in the larger tube. From the point of view of magnification it may be expected that an image at the high voltage side will generally be more magnified if the smaller electrode is on that side.

All electron lenses which have been discussed so far are two-electrode lenses. This implies that the potential of the object space is different from that of the image space. The two-electrode

*** Equipotentials of an unsymmetrical two-tube lens are drawn in Fig. 7.1 of Chapter vii.**

lenses are analogous therefore to glass optical immersion lenses. Multielectrode lenses belong to the same class if the potential of any intermediate electrode ranges between the potentials of the two adjacent electrodes. For example, in Fig. 4-3/2 is shown a three-tube lens in which the potential of the intermediate tube V_2 is variable and lies between the potentials of the first and of the last tube $(V_1 < V_2 < V_3)$. It will be observed that the focal lengths of such three-tube lenses are somewhat larger than the focal lengths of the corresponding two-tube lens with the voltage ratio V_3/V_v As a development from the three-tube lens, still more small intermediate tubes can be inserted. In this way the "lens chain" is obtained, by which electrons may be accelerated or decelerated with a relatively small focusing action. The extreme case of a lens chain is an insulating tube sprayed with a very thin metal layer. The resistance of this layer is large enough to maintain a linear potential drop from one end of the tube to the other. Such an arrangement produces a very nearly homogeneous field; it has actually been used to accelerate electrons without focusing them (F. 1), so that the focal length has in this case become infinite.

A completely new situation arises if the voltage of the intermediate electrode of a three-electrode lens is adjusted to be outside the range V_1 to V_s. Lenses belonging to this class are called "saddle field lenses", because the potential distribution becomes saddle-shaped, as will be pointed out in detail later on.

It appears that the focal length of a saddle-field lens is shortened gradually as the voltage V_2 of the intermediate electrode either increases beyond V_3 or decreases below V_1 Thus the focal length of the lens can be controlled within a very large range by varying V_2 for any constant value of V_3/V_1 A case of practical interest arises if $V_3 = V_1$ The equivalent electron lens is then surrounded by media of the same refractive indices at both sides, and corresponds to an isolated glass lens, so that in the literature it is often called an "einzel"-lens (i.e. single lens) (B. 11). Einzel-lenses consisting of three circular diaphragms have been investigated very thoroughly by H. Johannson and

O. Scherzer (J. 2). The special type of einzel-lens which has received particular attention is shown in Fig. 4.4. In Fig. 4.5 the focal length of such a system is plotted as a broken curve,

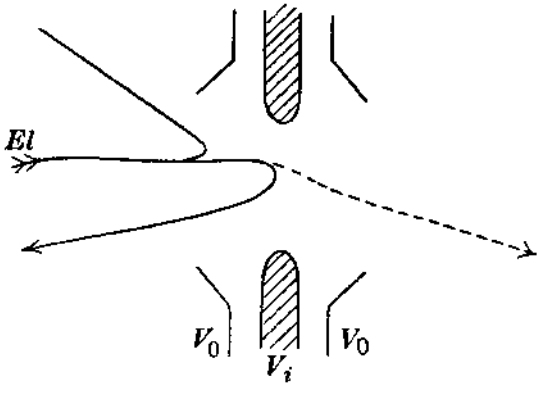

Fig. 4·4. Einzel lens.

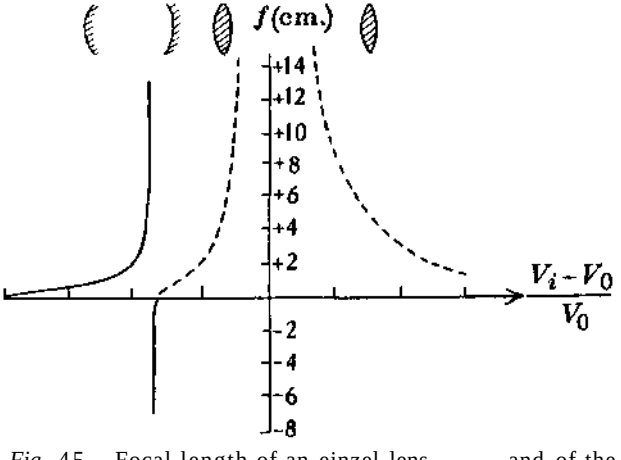

Fig. 45. Focal length of an einzel lens———, and of the corresponding electron mirror—.

against the ratio $\frac{V_i - V_o}{V_o}$, V_0 being the common potential of the two outer electrodes and V_i that of the inner. The two focal lengths f and f' have identical values, since the system is perfectly symmetrical. The focal lengths are of course infinite

when $V_1 = V_0$, i.e. $\frac{V_i - V_0}{V_0} = 0$. The focal length decreases rapidly as the difference $|Vi - V_0|$ increases, but the lens is always a converging lens, i.e. the focal length is always positive whether $\frac{V_i - V_0}{V_0}$ is positive or negative.*

A special case of some practical interest arises when the potential of the intermediate electrode of an einzel-lens is the same as that of the cathode of the whole arrangement. The einzel-lens is then operated with one voltage only and may therefore be called a "univoltage" lens.† As an example of this type of lens we may discuss a tube lens with an electrode arrangement similar to that shown in Fig. 4.3 *h*, all three tubes having equal radii. The intermediate tube is kept at cathode potential, so that $V_2 = 0$, and the positive potentials of the two external tubes are always equal, so that $V_1 = V_3$. If the emission velocity of the electrons from the cathode is negligible in comparison with V_1 the focal length of the univoltage lens does not depend on the voltage of the two external electrodes, the voltage ratio V_1/V_2 always being infinite. It is a merit of the univoltage lens that it needs the supply of one voltage only and that its focal length does not change if the voltage suffers large fluctuations. On the other hand, the focal length depends largely on the dimensions of the intermediate electrode, as can be seen from Fig. 4.6, where the midfocal length of the symmetrical three-tube univoltage lens is plotted against the length of the intermediate tube. If this lens is used in an apparatus where a given focal length is required, the dimensions of the electrodes must be adjusted with sufficient precision.

The saddle-shaped potential distributions of the symmetrical three-tube univoltage lens are shown in Figs. 47 *a* and 47 *b*. In order to show the equipotentials on a sufficiently large scale,

* The corresponding voltage ratios $\frac{V_i}{V_0}$ and $\frac{V_0}{V_i}$ are often called "normal", if $V_i > V_0$, and "inverse", if $V_i < V_0$.

† Epstein (E. 1) uses the general term "univoltage lens" for all einzel-lenses.

only one quadrant of the whole field plot is drawn in each of these two figures. The pictures are symmetrical about the midplane M and about the axis of rotational symmetry z. L_2 represents one-half of the intermediate tube and L_3 one of the two external tubes. Near the intersection of the midplane and the z-axis, the equipotentials are symmetrical hyperbolae. The asymptotes are two singular equipotentials which cross on the axis, they represent cones which are coaxial with the lens axis, having a semivertical angle $\gamma = 54.6°$. This angle is indicated in

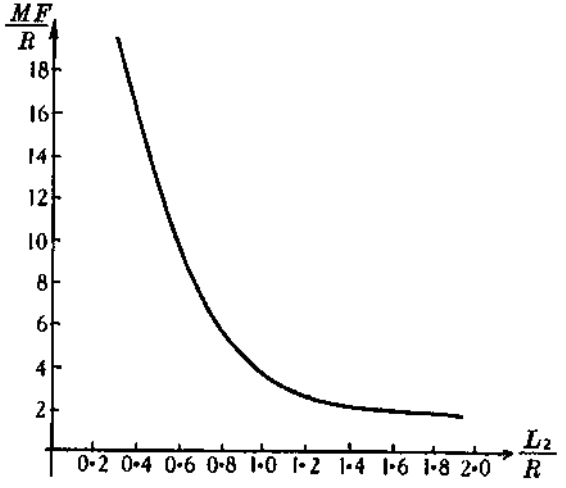

Fig. 4.6. Midfocal length of the three-tube univoltage lens.

Fig. 47 and it is remarkable that it does not depend on the shape of the electrode. The shape of the equipotential can be found from measurements in the field-plotting trough, but, since the potential gradient near the saddle point (i.e. near the point where the electrons cross over) is relatively small, it is generally difficult to define the field there by experimental methods. It is therefore most fortunate that it is possible to calculate this special field as a particular integral of Laplace's equation (3.2) (see, for instance, B. 11, p. 65).

Paraxial electrons in an einzel-lens such as the univoltage lens, with $V_2 < V_1$ have to climb up a path in the potential mountain.

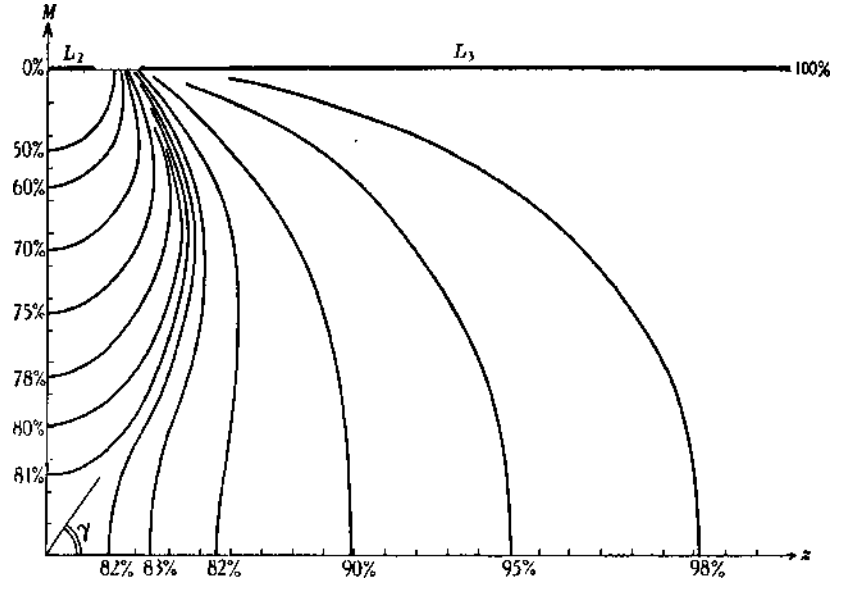

Fig. 47*a*. Symmetrical saddle shaped potential distribution.

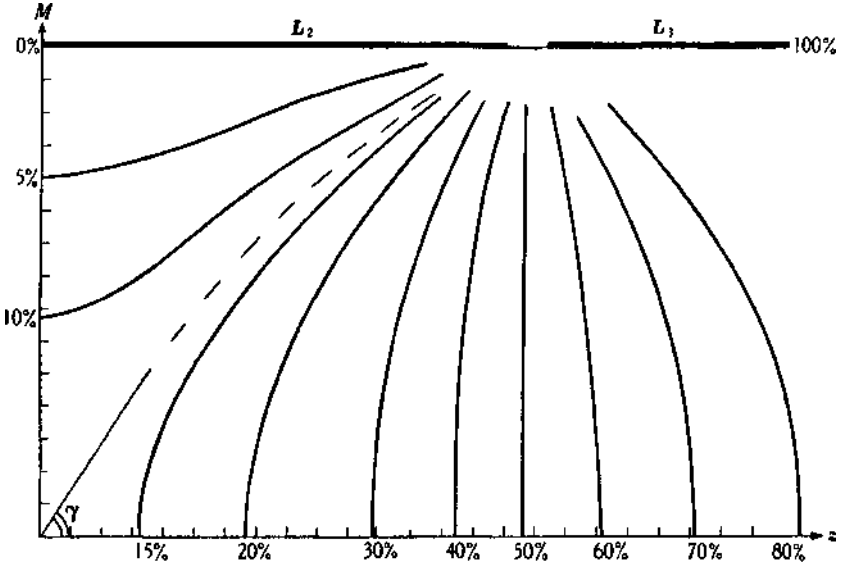

Fig, 47*b*. Symmetrical saddle shaped potential distribution.

The saddle-shaped field is like a pass over the mountain, the greatest height of the pass being the saddle point, but even there the electron is flanked on both sides by still greater heights. The altitude of the highest point on the pass, i.e. the voltage of the saddle point, depends on the voltages and the geometry of the electrodes. In the example of the symmetrical three-tube univoltage lens it depends on the length of the intermediate electrode and on the common voltage of the two external electrodes only.

In this symmetrical lens, the saddle point lies exactly in the midplane. That is no longer the case, however, if either the geometry or the potential of the electrodes becomes unsymmetrical. The saddle point then shifts along the axis and stays always at that side of the midplane where the potential gradient is the largest. The position of the potential saddle near to a charged straight diaphragm has been investigated experimentally and theoretically by A. Glaser and W. Henneberg (G. 3). Suppose the field strengths on both sides of the diaphragm in the case when the aperture is closed are E_1 and E_2. Then the distance s of the saddle point from the aperture, measured in terms of the aperture radius R, can be tabulated as a function of the ratio of the weaker field E_1 to the stronger field E_2. The following five values may be given as an example:

s/R	0	0.2	0.5	1	3
E_1/E_2	100%	60%	29%	16%	1%

In Fig. 4.8 *a* is shown a potential distribution round the aperture, in the case where the ratio E_1/E_2 is 1.4 %. It should be emphasised that the sign of the two field vectors E_1 and E_2 has to be opposite if a saddle field is to be expected. If E_1 and E_2 are of the same sign, they may be very different, but no saddle-shaped potential distribution will result. The potential distribution which will be produced by unequal but equidirected E_1 and E_2 is illustrated in Fig. 4.86. The equipotentials penetrate the aperture to a considerable extent but none of them cross; just one singular

equipotential being observed reaching the diaphragm electrode at right angles.

With respect to the einzel-lens with negative potential at the inner electrode, it must be remembered that the potential of the saddle point must never be negative with respect to the cathode potential, since in order to pass the ridge, the electron must retain some kinetic energy even at the top.

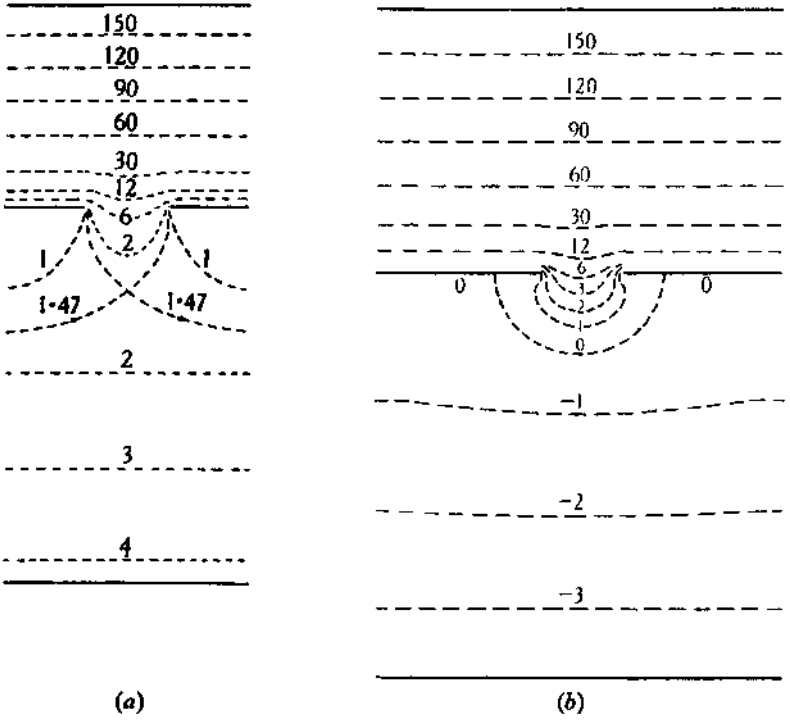

Fig. 4.8. Field penetration through an aperture: *(a)* fields *in* opposite directions; *(b)* fields in the same direction.

If the potential of the intermediate electrode is gradually made more and more negative, the path of the electrons will finally be blocked and all those moving up the potential mountain will be returned. At first the marginal electrons are returned, but when the inner electrode becomes still more negative, the axial electrons are also reflected. In this way the einzel-lens can be used to modulate the intensity of an electron beam, as if

the lens were closed by an iris diaphragm when the negative voltage *Vi* is increased.*

If the electrons emitted by any extended object are projected backwards by such a reflecting axially symmetrical field, a most marvellous phenomenon can be observed. Under certain conditions, the reflected electrons form a real image. This was predicted theoretically by W. Henneberg and A. Recknagel (H. 5) and was verified later by G. Hottenroth (H. 7). The arrangement acts like an electron mirror. By changing the voltage at the negative electrode, different equipotentials can be chosen to act as a reflector. Thus the focal length and the principal plane of the mirror can be varied. In Fig. 4-5 a solid curve shows the focal length of the electron mirror produced by the electrode arrangement of Fig. 4-4. This focal length at first increases with decreasing negative bias, then suddenly it assumes negative values, which means that the mirror reflects the electrons like a concave glass optical mirror.

A simple type of electron mirror is produced by the electric field between two tubes. F. H. Nicoll (N. 1) published recently some interesting details of this two-tube mirror obtained in a very convenient experimental arrangement. The scheme of the measuring apparatus is shown in Fig. 4.9. There, the electron beam *El* illuminates the wire gauze object *W* and the electron lens L, consisting of two tubes with the voltages V_0 and V_1 projects an electron image I of the gauze. The position of the image I depends on the voltage ratio of the lens, and can be calculated according to the data given in Figs. 4.1 and 4.2; the position of principal planes and focal points of the lens *L* is known as a function of this voltage ratio V_1/V^ The image I serves as an object for the electron mirror *M* which is formed by the electric field produced by the two tubes with the voltages V_1 and V_2. The mirror *M* projects the electrons emitted from the "mirror-object" / into a "mirror-image" which can be detected

*** In Gaussian optics, all electrons should have equal axial velocities independent of their axial distance. Thus either all electrons should be transmitted or reflected simultaneously. The finite slope of any actual modulator characteristic is due to lens errors.**

with a fluorescent screen *S* on the movable target *T*. The pictures at the fluorescent screen are observed by looking "through" the electron mirror. The target contains a small aperture *A* in its centre which is sufficient to let through the electrons coming from *W* and forming the mirror-object I, but is narrow enough to cut out only a very small central fraction of the image produced by the mirror.

The behaviour of the electron mirror can generally be judged from the shape and position of the reflecting equipotential. At the moment of reflexion, the velocity of the paraxial electrons is reduced to zero. Thus the reflecting equipotential is at cathode

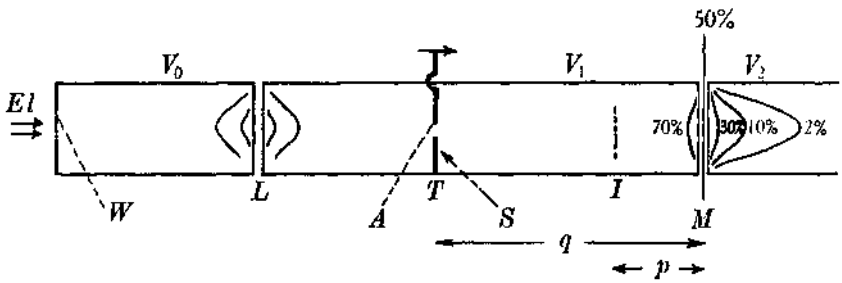

Fig. 49. Two-tube electron mirror.

potential and it is often called the "zero equipotential". For the present purpose it is again suitable to label the equipotentials as in Fig. 3*2 in terms of percentage of the total potential difference. In the present arrangement, V_1 is positive and V_2 is negative with respect to the cathode, so that the zero equipotential of the electron mirror is equivalent to the equipotential labelled

$$\frac{100}{(1 - V_1/V_2)}\ \%. \qquad (4.4)$$

Some of these equipotentials are shown in Fig. 4.9 with the proper designation.

In Fig. 4.10, object distances and magnifications are plotted as functions of the voltage ratio (— V_1/V_2). For any voltage ratio V_1/V_2, the corresponding reflecting equipotential, according to

formula (4.4), is noted there. For the curves of Fig. 4.10, the target *T* was fixed at two different image distances *(q = MT)*, the broken curves corresponding to $q = 2R$ and the solid curves to $q = 22R$, R being the radius of the tube electrodes. In the

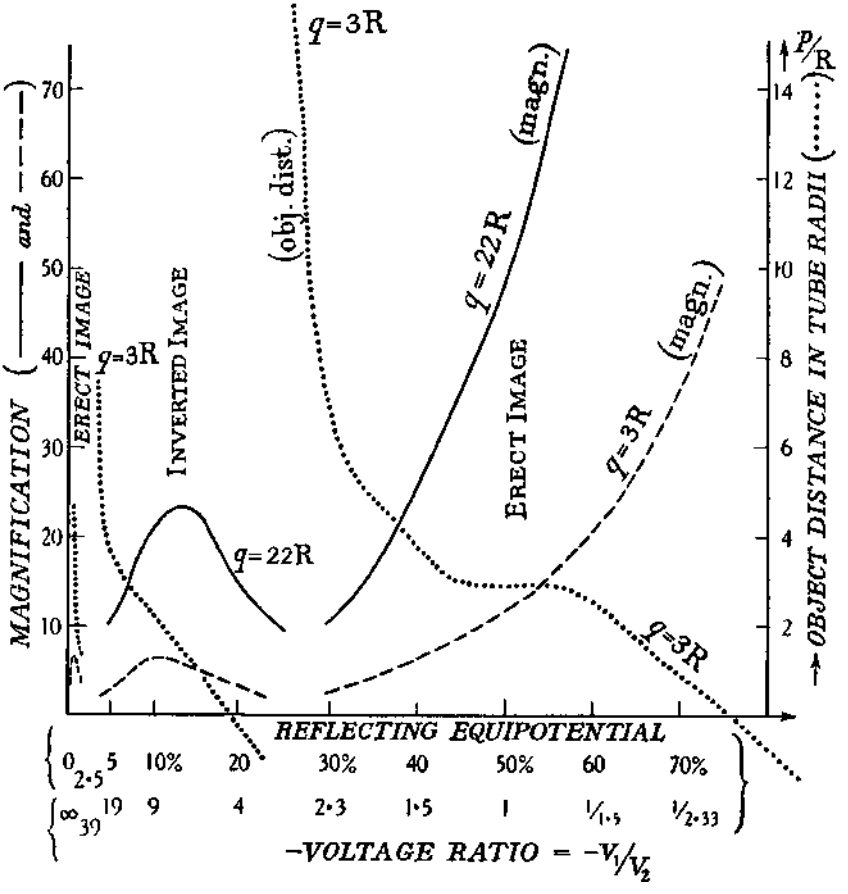

Fig. 4.10. Magnification by the two-tube mirror.

measurements, fixed values of the voltage ratio V_1/V_2 of the electron mirror were arranged so that by varying the voltage ratio V_1/V_0 of the lens L, the position of I was controlled, i.e. the mirror-object distance p = *MI* was varied until the image at the screen *S* on the target *T* appeared to be in focus. Then the

magnification could be measured; it is plotted in the diagram of Fig. 4.10.

When the value of V_1/V_2 is gradually changed from —1/3 to — 1.5, the surface where the reflection takes place gradually changes from the 75% to the 40% equipotential. Within this range of V_1/V_2 the mirror object is virtual for the two fixed image distances of Fig. 4.10, and the mirror projects an erect image. The mirror reduces the convergence of the incident electron beams and thus acts like a convex glass mirror.

If the reflecting surface changes from the 40% to the 30% equipotential, corresponding to a decrease of V_1/V_2 to —2.5, the distance of the mirror object from the midplane increases to infinity whilst the magnification decreases. Proceeding to still smaller values of the reflecting equipotential, the mirror will project an inverted image corresponding to a real mirror object. If these values are still further decreased, the object again moves off to infinity. At $V_1/V_2 \quad -20$ (5% equipotential), the field between reflecting equipotential and fluorescent screen is powerful enough to converge the beams again after a first cross-over, so that an intermediate image is produced, and at the fluorescent screen a second image is detected. With still larger values of $(-V_1/V_2)$ this process is repeated as the beam crosses over more and more times until finally space charge in the low velocity region of the mirror and increased aberrations prevent the formation of a well-defined image.

All the pictures produced by the electron mirror show a surprisingly good definition. Thus it seems possible that the mirror might be applied as a useful element of construction of electron optical apparatus. Moreover, there are distinct possibilities of using the mirror even for improving the performance of electron lenses, with a view to correcting the errors of distortion and of chromatic aberration. However, a discussion of this matter will be postponed for later chapters.

Chapter V

MAGNETIC ELECTRON LENSES

The acceleration which an electron receives in a magnetic field is in a direction perpendicular to the field vector and to the velocity of the electron. A static magnetic field does not change the kinetic energy of the electron, but only changes the curvature of its path. Equating the magnetic force to the centrifugal force of the electron one obtains

$$euH = \frac{mu^2}{\rho}, \tag{5.1}$$

e and *m* being charge and mass of the electron, *u* its linear velocity, *H* the magnetic field strength and *p* the radius of curvature of the path.

If the electron moves in a direction perpendicular to a homogeneous magnetic field, its path is a circle. If it moves parallel to the direction of the magnetic field, it is not influenced and travels along a straight line. If the electron moves through the homogeneous magnetic field in a direction making an angle *0* with the lines of force, the velocity *u* can be imagined to be split up into two components. The first component

$$u_x = u \cos \Theta \tag{5.2}$$

is parallel to the field and is not influenced by the field. The action of the field on the other component

$$u_y = u \sin \Theta, \tag{5.3}$$

which is perpendicular to the field, will not depend on the existence of the first component. Thus the projection of the electron path on a plane perpendicular to the lines of force must be a circle and the path of the electron itself must be a spiral lying in the wall of a cylinder.

The time t which the electron takes to perform its circular movement is obtained from (5.1):

$$\left.\begin{aligned} \frac{e}{m} H\rho = u_y = \frac{2\pi\rho}{t} \\ t = \frac{2\pi}{H}\frac{m}{e} \end{aligned}\right\} \qquad (5.4)$$

It is remarkable that this time is independent of u, Θ, and of p. Superimposed on the circular movement is the longitudinal movement. During the time t the electron moves a distance / in the longitudinal direction, given by

$$l = u_x t = (u \cos \Theta)\frac{2\pi}{H}\frac{m}{e}. \qquad (5.5)$$

Suppose a number of electrons of given velocity u cross any given line of force at a point / at a number of different inclinations & > assumed to be so small that cos $\Theta \approx 1$. All these electrons will again cross the same line of force at another common point I', because the component perpendicular to the line of force performs just one full revolution within the time t, given by eq. (5-4). Thus it appears that a homogeneous magnetic field is able to produce an electron optical picture of unit magnification within a distance l_n from the object, l_n being equal to / as given by eq. (5.5), or a multiple of l which is perfectly defined by the ratio of the electron velocity u and the magnetic field strength. The focal length of the homogeneous field is infinite, thus, optically, it belongs to the telescopic systems.

It may seem difficult to understand the motion of the electron in a magnetic field from an optical point of view. The difficulty is due to the fact that the refractive index of the beam is not a simple function of the geometrical co-ordinates only, but, as follows from the above considerations, it also depends on the direction of the beam. Such a problem is not new. In crystal optics methods have been developed to deal with refraction in anisotropic media, and W. Glaser (G. 2) worked out the theory of magnetic lenses on corresponding lines.

The whole problem of the refraction of electrons in magnetic fields can, however, be attacked in a much simplified way if the two-dimensional motion of the electron in a meridional plane is considered.* This meridional plane rotates with the electron round the axis of the lens; the angular velocity of rotation is of course not constant, but depends on the radial distance of the electron from the axis and on the intensity and the distribution of the magnetic field. Any change of direction of the electron beam in the meridional plane, may be ascribed to a change of a hypothetical "refractive index" or of a hypothetical "potential" in this meridional plane. This potential may be called the "meridional potential". As the problem of refraction is now a two-dimensional one only, the new refractive index does not depend on the direction of the electron beam.

The existence of such a refractive index has repeatedly been stated in the literature and its magnitude has been derived from Maxwell's equations (S. 6, D. 4, B. 11). These calculations, however, are simply applications of electromagnetic theory and are outside the scope of this tract. All that is intended here is to give a physical picture of the facts and to interpret the formulae which are needed for quantitative investigations.

The meridional potential can be considered as a two-dimensional scalar potential and its equipotential lines can be drawn in the meridional plane. In eq. (i-6), it was stated that the electrokinetic force is a function of the electron velocity and of the magnetic vector potential only, so that the new meridional potential will only contain these two variables. In the axially symmetrical fields of electron lenses the problem is simplified, because the magnetic vector potential follows circular lines round the axis and becomes zero on the axis. C. Stormer (S. 6), J. Dosse (D. 4) and others (B. 11) have shown that the meridional potential Q is given by

$$Q = V - \frac{m}{2e}\left(\frac{C}{r} - A\right)^2, \qquad (5.6)$$

*** The author is indebted to Mr C. P. Singer for many helpful discussions on the following theory of the magnetic lenses.**

V being the kinetic energy of the electron measured in E.M.U. and A being the magnetic vector potential. The first term in the bracket is given by

$$C/r = A - m/er\dot{\psi}, \tag{57}$$

r being the radial co-ordinate of the electron and the angular velocity of the rotating meridional plane. It is a most remarkable fact that C assumes a constant value for all skew electron rays and becomes zero for axial rays. Thus, for the latter case, eq. (5.6) may be rewritten in the form

$$A = \sqrt{\frac{2m}{e}(V - Q)}, \tag{5.8}$$

showing that then the equipotentials of A are also equipotentials *of* Q.

Generally, the vector potential A is not directly measurable, but in a magnetic field with axial symmetry, as in the electron lenses, all relations are appreciably simplified and A is then directly proportional to the magnetic flux. The general definition of A in terms of the magnetic field strength is

$$H = cml A, \tag{5.9}*$$

and if this is introduced to Stokes* equation we have

$$\int H_z dS = \int \text{curl } A . dS = \oint A . dl. \tag{5.10}$$

The integral of the axial component of the field over a surface is equal to the line integral of the vector potential round the boundary curve of this surface. In our case the boundary curve

*** The non-mathematician may gain an indication of the properties of the curl function by thinking of the relation between the magnetic field H and the corresponding electric current 1. Just as the magnetic lines of force run in circles round a cable carrying a current, so the magnetic vector potential runs *in* circles round the magnetic line of force. In the magnetic electron lens the vector potential is arranged in concentric circles round the axis, just as the magnetic lines of force would be arranged inside a thick copper conductor.**

is a circle and on account of the rotational symmetry A is constant along it. Thus the flux (eq. (5.10)) becomes:

$$2\pi\int H_z r\,dr = 2\pi r A \qquad (5{\cdot}11)$$

and

$$A = \frac{1}{r_0}\int_0^{r_0} r H_z\,dr. \qquad (5{\cdot}12)$$

By means of eq. (5.12) it is possible to obtain A (for instance, by graphical methods) when the axial component of the magnetic field strength has been measured (for instance, by means of a search coil).

As an example of the electron optical method we may treat again the homogeneous field which was discussed from the

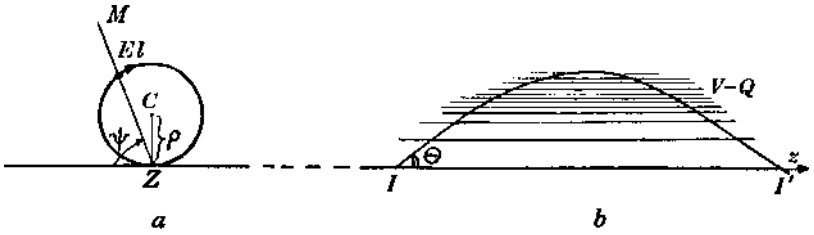

Fig. 5.1. Motion of an electron in a homogeneous field, *(a)* Radial component; *(b)* motion in the rotating meridional plane.

electron mechanical point of view at the beginning of this chapter. For H= const, it follows from eq. (5.12) that $A = Hr/2$, the surfaces of equal vector potentials being coaxial cylinders cutting the meridional plane in straight lines. The meridional plane is shown in Fig. 5.16. Along the z-axis the vector potential A is zero, thus the relative meridional potential of an axial electron at the axis, according to eq. (5.8), is given by $(V— Q)$ = o so that there $V=Q$. Some straight lines of equal A are drawn in the meridional plane. According to eq. (5.8) they are also equipotentials of $(V— Q)$. As A increases with increasing distance r from the axis, so also does $\{V—Q)$. An electron moving away from the axis has to climb up the potential mountain in the meridional plane and is refracted at the $(V—Q)$ equipotentials according to Snell's law, just as for the case of the electrical equipotentials

explained in Chapter III. If an electron beam cutting the axis at I is traced through the meridional plane, it will cut the axis again at I ' , where I I ' is identical with the distance I given in eq. (5.5). In Fig. 5.1 *a* there is shown the radial component of the movement of the same electron. According to eq. (5.1) this component is a circle with radius *p* and centre C. The z-axis is perpendicular to the plane of the drawing through the point *Z*. The meridional plane M, containing the electron

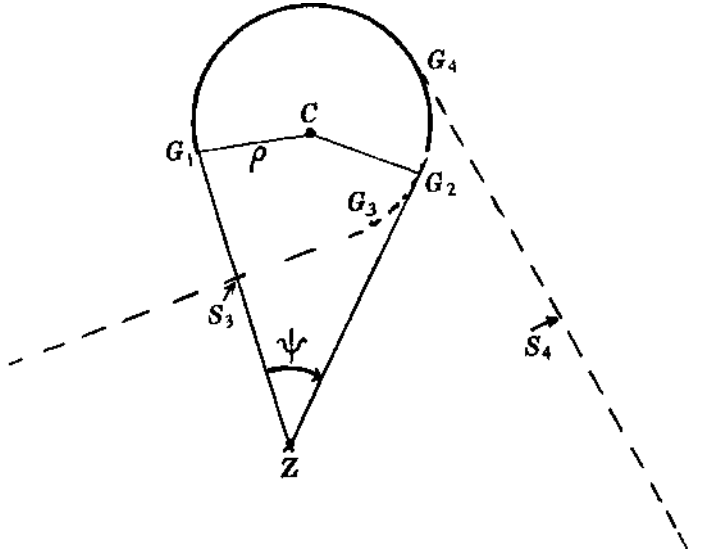

Fig. 5*2. Radial component of an electron path in a hypothetical short homogeneous field.

El, rotates round the z-axis and makes an angle *xjr* with its original position. This original position is taken when the electron orbit intersects the z-axis at I and again at i [7] .

The radial component of the motion through a hypothetical short homogeneous field is shown in Fig. 5.2 (H. 8). The electron, starting from the axis in a field-free space, travels along the straight line ZG_1 At G_1 it suddenly enters the homogeneous field and describes a circle with radius *p* round the centre C, at G_2 it leaves this field suddenly and returns in a straight line G_2Z to the axis Z. From the figure it is, obvious that unless this

tangential line passes through Z a definite image will not be obtained. The electron can only return to the axis if object and image are symmetrically placed with respect to the field. In all other cases, the electron path would become skew and would never meet the axis again. This is indicated by the dotted lines for two hypothetical fields breaking off at G_3 and at G_4 respectively. In their meridional planes, these rays would approach the axis in hyperbolical curves. The nearest distances to the axis would be reached at S_3 and S_4 respectively, and from there on the two rays would go off again to infinity.

In nature a magnetic field cannot begin or end suddenly in space without introducing a large radial component which

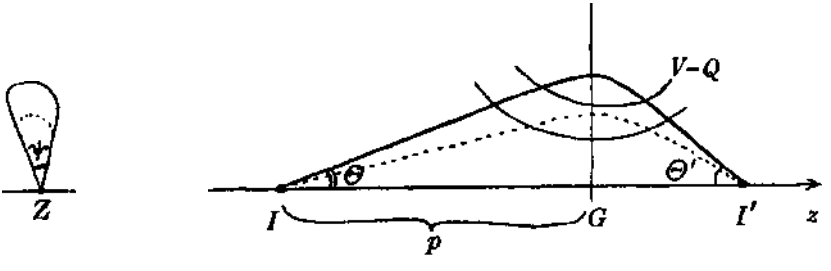

Fig. 5.3. Focusing action of a magnetic coil, *(a)* Radial component; *(b)* motion in the meridional plane.

modifies the electron motion. Because the rotational symmetrical field is free of magnetic poles (div H=o), any decreasing field must contain a radial component which is proportional to the distance from the axis. As W. Glaser (G. 2) pointed out, this is an essential condition for the production of an optical image by a magnetic lens.

H. Busch (B. 13) has first clearly established the theory of the short magnetic lens. We shall here discuss this problem, following the lines of a simplified analysis which is due to A. Bouwers (B. 5).

As shown in Fig. 5.3 *a* and *b,* an electron starting on the axis at a point I travels along a substantially straight path until it enters gradually a magnetic field which extends round an

equatorial plane G and which decays rapidly along both directions of the axis of rotational symmetry z. To give an impression of the shape of the meridional equipotentials two such lines of equal (F — Q) are drawn in Fig. 5.36. The electrons are deflected gradually in the field and then proceed to the substantially field-free space, where they travel along straight lines, and finally intersect the axis at I'. For a given object distance I $G = p$ the position of the image I' does not depend on the slope angle 0 so long as cos Θ~i.

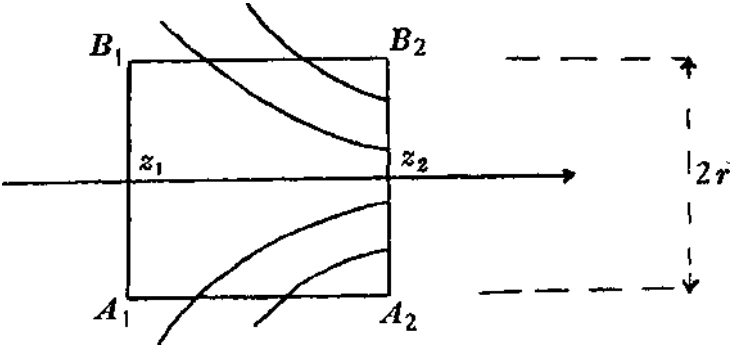

Fig. 5*4. Magnetic lines of force in a small coaxial cylinder.

The properties of the inhomogeneous magnetic field may be explained with the aid of Fig. 5.4. There A_2B_2 and A_1B_1 are two identical small circular cross-sections perpendicular to the axis z of the coil through the points z_2 and z_1 The number of magnetic lines of force passing through the cross-section (2), but not passing through the cross-section (1), is

$$\pi r^2(H_2 - H_1).$$

This must be equal to the number of lines of force penetrating the cylinder wall of surface area

$$2\pi r(z_2 - z_1),$$

so that the mean value of the radial magnetic field is

$$H_r = \frac{r(H_2 - H_1)}{2(z_2 - z_1)}.$$

If the distance $z_2 - z_1 = dz$ is made vanishingly small this becomes

$$H_r = \frac{r}{2}\frac{dH_z}{dz}. \qquad (5{\cdot}13)$$

Consider now an electron moving with a velocity component u parallel to the Z-axis at a distance r. The radial component H_r of the field will act upon it with a force in the lateral direction given by

$$\frac{md(r\dot{\psi})}{dt} = euH_r. \qquad (5{\cdot}14)$$

The radial velocity component

$$\dot{r} = u \sin \Theta = \frac{ur_{\max}}{p} \qquad (5{\cdot}15)$$

is supposed to be small, where H_z is also small, at the point where the electron enters the magnetic field, and it becomes zero when the electron is at the maximum distance r_{max} from the axis. Therefore, the force due to r and H_z may be neglected as a first approximation.

The acceleration in the lateral direction is obtained from eqs. (5.13) and (5.14):

$$\frac{d(r\dot{\psi})}{dt} = \frac{eru}{2m}\cdot\frac{dH_z}{dz}. \qquad (5.16)$$

By integration between — and z, after substituting $dz/u = dt$, one finds the lateral velocity:

$$r\dot{\psi} = \frac{er}{2m}H_z \qquad (5{\cdot}17)$$

and with $dz/u = dt$

$$\psi = \frac{e}{2mu}\int_{-\infty}^{\infty} H_z dz. \qquad (5{\cdot}18)$$

Expressing the electron velocity in equivalent volts, V_{voit}, and the magnetic field H in gauss, the angle of rotation expressed in radians becomes

$$\psi = \frac{0{\cdot}15}{\sqrt{V_{\text{volt}}}}\int_{-\infty}^{\infty} H_z dz. \qquad (5{\cdot}19)$$

If the electron travels in the same direction as H_z, has to be taken clockwise on looking in the direction of H_z.

The inward force, accelerating the electron towards the axis, must be in equilibrium with the centrifugal force, which is seen from eq. (5.17) to be

$$\frac{m(r\dot{\psi})^2}{r} = \frac{e^2 r}{4m} H_z^2. \qquad (5{\cdot}20)$$

The corresponding acceleration is therefore

$$\ddot{r} = \frac{e^2 r}{4m^2} H_z^2. \qquad (5{\cdot}21)$$

Integrating and putting $dt = dz/u$, one obtains the final inward speed:

$$\dot{r} = \frac{u r_{\max}}{p} + \frac{e^2 r}{4m^2 u} \int_{-\infty}^{\infty} H_z^2 dz; \qquad (5{\cdot}22)$$

the object distance p and the elongation r_{max} define the initial conditions. With the inward speed r the electron will meet the axis after a time $t = r/r$. For p (beam entering parallel to the axis) the path ut is the focal distance

$$f = \frac{ur}{\dot{r}} = \frac{4m^2u^2}{e^2 \int_{-\infty}^{\infty} H_z^2 dz}. \qquad (5{\cdot}23)$$

This is the famous formula of Busch. Expressing again the electron velocity in equivalent volts, V_{volt}, and the magnetic field H in gauss, the power of the magnetic lens in cmr[1] becomes

$$\frac{1}{f} = \frac{0{\cdot}022}{V_{\text{volt}}} \int_{-\infty}^{\infty} H_z^2 dz. \qquad (5{\cdot}24)$$

For large electron velocities, due to the relativistic increase of the mass of the electron, the actual focal length f_{rel} is larger than that given by eq. (5.24). F. Ollendorf and G. Wendt (O.1) calculated

$$f_{\text{rel}} = f\left(1 + \frac{KV}{1000}\right), \qquad (5{\cdot}25)$$

KV being the electron velocity expressed in equivalent kilovolts.

In electron microscopy (Chapter vn) in some cases electrons up to 100 kilo volts are focused by magnetic lenses. In these cases the actual focal lengths of the lenses may be 10% larger than those calculated from the ordinary Busch formula.

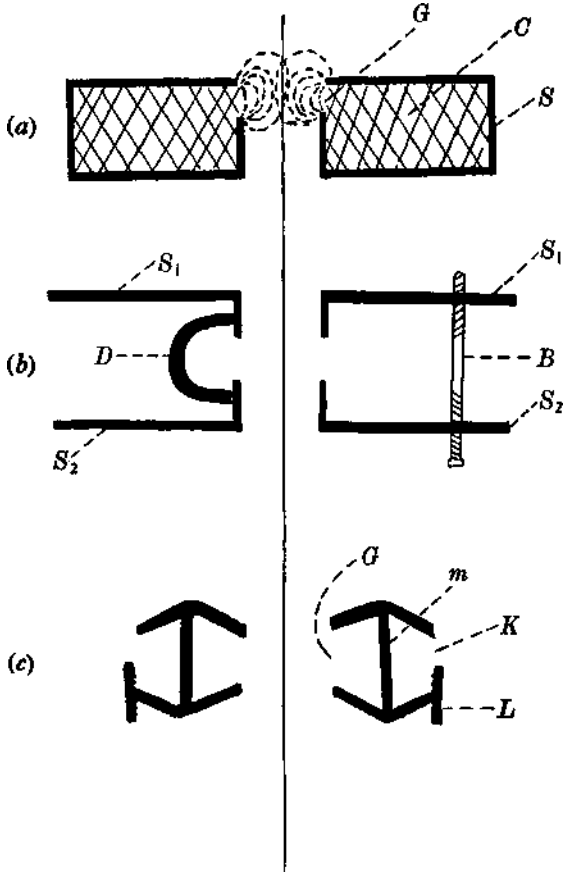

Fig. 5.5. ***(a), (b), (c)*** **Magnetic lenses.**

Experimentally, the axially symmetrical magnetic fields are produced by ordinary electric coils, by iron-shielded coils, or by permanent magnets. An example of an iron-clad coil is show in a meridional cross-section in Fig. 5.5 *a*. The mild iron shield *S* completely surrounds the coil C, leaving only a relatively small annular gap G. The total flux passing through the iron.

has to cross this gap. It produces an intense stray field by which the electrons are focused. Fig. 5.56 shows a possible form of a permanent magnetic lens which was designed by F. H. Nicoll. Here the two iron parts S_1 and S_2 are kept in position by three brass bolts *B* spaced within a distance of 120° over the equatorial cross-section. Half-way between these bolts, there are arranged

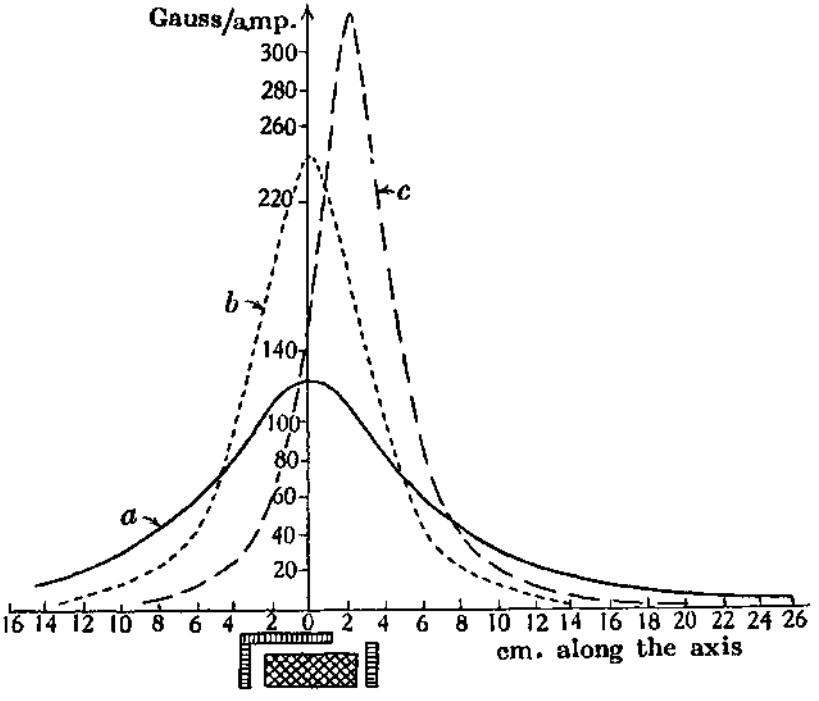

Fig. 5.6. Field distribution of magnetic lenses along their axes.

three equidistant horse-shoe magnets *D* bridging the gap of the two iron parts. In this way the total flux produced by the horse-shoe magnets passes the gap in the form of a stray field. This field is found to be well distributed over the whole gap so as to generate a field of good axial symmetry. The width of the gap can be changed by tightening or loosening the three bolts *B*. In this way the field intensity and distribution can be altered and the focal length of the lens can be controlled. Fig. 5.5 *c* shows another

type of permanent magnetic lens (F. 2). The cylindrical magnet *M* is surrounded by two pole shoes, one with the gap *G* producing the stray field which focuses the electrons. The other pole shoe has the gap *K* which can be more or less shunted by the iron cylinder L, screwed across it. In this way the flux across

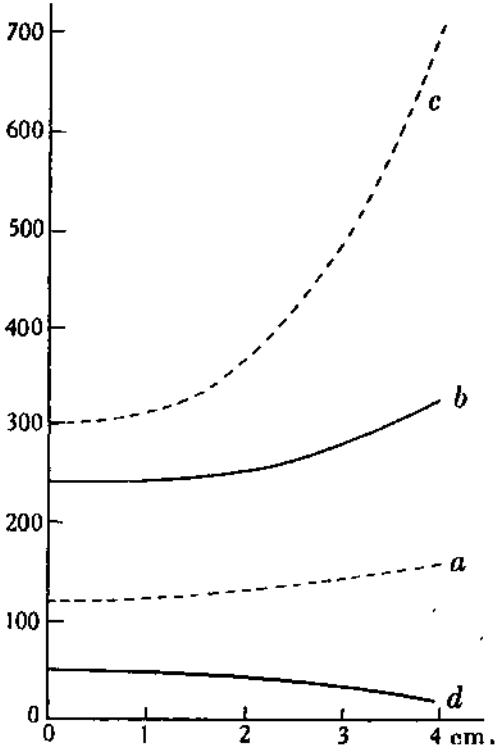

Fig. 57. Radial field distribution in magnetic lenses.

G can be changed and the focal length of the lens can be controlled.

Some examples of actually measured field distributions are shown in Figs. 5.6 and 57 (K. 2). The field strength along the axis is shown for different electron lenses in Fig. 5.6. Curve *a* shows the field distribution for a simple air coil not containing any iron and with about 1500 turns of copper wire. Curve *b* refers to this coil if its ends and outer cylindrical wall are covered

by iron plates, only the inner cylindrical surface is left uncovered, representing the magnetic gap. Curve *c* shows the field distribution if the inner cylindrical wall of this coil is also covered by an iron plate leaving open a small gap of only one-third of the length of the wall. The centre of the coil is chosen in each case as the zero point of the axis. It may be noticed that generally the field decays to 10% of its maximum value within a distance of about one mean coil radius for iron-clad coils and within a distance of roughly two mean coil radii for air coils. The decay of the field is roughly exponential.

The magnetic field strengths along the radii of the above coils are shown in Fig. 5.7. The curves *a, b, c* belong again to the air coil, the iron coil with wide gap and to the iron coil with small gap, respectively. Curves *a* and *b* were measured along a radius through the centre of the coil. For curve *c* the measurements were taken through the middle of the gap, which is displaced from the centre of the coil. All curves show increasing values of the field strength with increase in radius. Curve *d* shows the radial distribution of the iron coil with the large gap at some distance from the centre of the coil. This curve shows a remarkable decrease of field for the peripheral regions.

The focal length of the magnetic lenses produced by the field distributions of Fig. 5.7 can be calculated by means of eq. (5.24). It appears that the focal length of the magnetic lens with a given coil current and a given electron velocity can be shortened by a factor of about 3 if an iron shield is used.

If for any iron-clad coil the coil current is decreased until its focal length equals exactly that of the corresponding air coil, the rotation of the electron image is found to be always larger for the air coil. This can be proved by a calculation from eq. (5.19), using curves such as those of Fig. 5.6. The rotation of the image is identical with the rotation of the midplane.

If a magnetic lens is "infinitely" short, the rotation of the image can be neglected and the image is therefore inverted as in the case of a glass lens. If the coil is infinitely long, the rotation is 180^0, as compared with the glass lens, and an erect image is

produced. Thus for an ordinary short lens the image rotation is between o° and 180^0; it is larger, the more the field is extended along the lens axis.

If a magnetic lens of a given focal length has to be designed, a general relation connecting the ampere turns *(A T)* of the coil with its focal length (f) is of some practical importance. E. Ruska (R. 4) has derived the following formula:

$$AT = 326S\sqrt{KV + \frac{(KV)^2}{1000}}\sqrt{\frac{R}{f}}, \qquad (5{\cdot}26)$$

where KV is the electron velocity in equivalent kilovolts, R is a mean radius of the coil and S is a factor depending on the special shape of the magnetic field. S is equal to unity for a circular linear conductor. For any extended air coil, S is generally not more than a few per cent larger than unity, but for iron-clad coils S may have only half the value it has for the corresponding unshielded air coil. Whilst S for a given air coil is strictly constant, it may change noticeably for a given iron-clad coil if the electric current through the coil is altered. This change is due to a change of the permeability of the iron which depends upon the absolute value of the magnetic field. Thus the field distribution is altered if the coil current is changed. According to eq. (5.26) the focal length f becomes shorter, the more the number of ampere turns is increased. S will, however, gradually increase with AT and the lower limit for the focal length for any electron velocity is given by the saturation of the ferromagnetic shield of the coil.

As to the position of the principal points, which in this case are identical with the nodal points, E. Ruska (R. 4) states that they are mostly crossed over with respect to their appropriate focal points and that they lie generally rather close to the centre of the magnetic field. About their accurate position or the change of this position with changing coil current no information is yet available.

Chapter VI

LENS ERRORS

The laws of Gaussian optics interpreting the behaviour of paraxial beams in electron lenses, which were developed in Chapter II, are only valid if the beams are so close to the axis that terms of higher order than the first in the expansion of the sine of the slope angles can be neglected in practically useful electron-optical systems. However, the apertures are generally so large that these paraxial rays constitute but a small fraction of the image-forming rays. In 1855 L. von Seidel extended the first-order theory by developing a trigonometrical analysis and by including the third order term in the sine expansion. In his third-order theory a series of five correction terms is applied to the first-order theory. These five terms, which characterise five independent lens errors, can also be developed in a completely different way from Hamilton's characteristic functions (S. 7, R. 2), showing that for the isotropic media of glass optics as well as of electrostatic electron optics there exist just these five and no more third-order aberrations for anisotropic refraction. However, as in magnetic fields, W. Glaser (G. 2) has shown that eight independent third-order errors have to be assumed.

Although the mathematical theories supply a logical basis for classifying the lens errors, they have so far been of little practical assistance for the design of corrected electron optical instruments.

The only systematic way of improving the correction of electron optical systems is to begin by measuring the lens errors separately either by direct methods or by tracing the rays through plots of equipotentials. Then, for electrostatic lenses, the arrangement and the shape of the electrodes, for magnetic

lenses, the arrangement of the current conductors and the shape of the iron shieldings, has to be altered with a view to improving the correction. General lines of attack for obtaining an improved performance of electron lenses have been given.

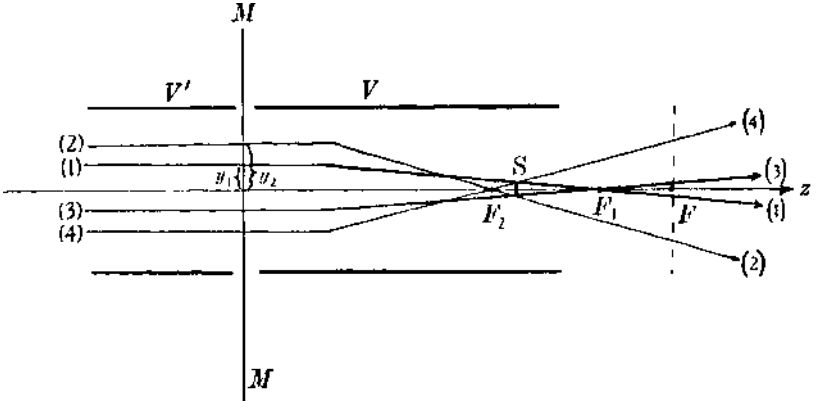

Fig. 6.1. Spherical aberration of a decelerating two-tube lens.

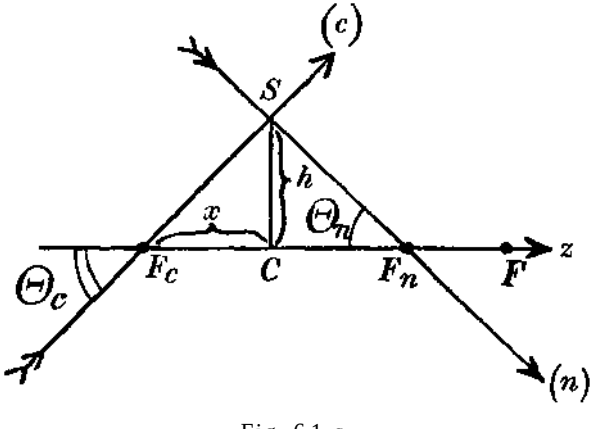

Fig. 6.1 *a.*

Very little quantitative research on the errors of electron lenses has, however, yet been carried out.

The five isotropic lens errors can be divided into one axial error and four field errors. The axial error, called spherical aberration, occurs if rays emitted from a point object on the

axis do not recombine to form a point image. Here, the extreme case when the object is at infinity is of principal interest, and it is therefore illustrated in Fig. 6-i by the example of a symmetrical two-tube lens. The axis of this lens is indicated by *z*, *M* ... *M* represents the midplane. Two pairs of parallel beams are drawn, the "zonal" beams (1) and (3), which are beams travelling at a "medium" distance y^1 from the axis, and the "marginal" beams (2) and (4), which are beams at a relatively "large" distance^ from the axis. Paraxial beams, which are not drawn in the figure, would be focused in the paraxial focus *F*. If the given lens shows remarkable spherical aberration, the focus F_1 of the zonal rays and F_2 the focus of the marginal rays are found to be different from the paraxial focus *F*. The distances FF_1 and FF_2 are called the longitudinal spherical aberrations of the beams (1) (3) and (2) (4) respectively. If, as in the given example, the focal length decreases with increasing aperture of the beam, the aberration is conventionally called a positive one. It is a rule of experience that the spherical aberration of electron lenses is generally positive.

Measurements of spherical aberration can be made by means of the apparatus already described in Chapter 11. A number of fine electron pencils emerging through a pepperpot-like diaphragm is traced through the actual electron lens by means of a sliding fluorescent target, and the paths of the beams are measured up with a calibrated microscope. A corresponding method is well known in glass optics under the name of the "Hartmann test".

The spherical aberration of any given semiaperture *y* changes with the voltage ratio of the lens. This is illustrated by Fig. 6-2, where the midfocal lengths of the symmetrical two-tube lens, decelerating parallel beams, are plotted against the voltage ratio. The parameters of the different curves correspond to the different semiapertures of the beams entering the lens, as noted in the figure. The beams of a given semiaperture are produced experimentally by means of a series of diaphragms having circles of holes of different radii. From Fig. 6-2 data can be taken

to draw the conventional types of aberration curve, as shown in Fig. 6.3, in which, for a given voltage ratio as parameter, the

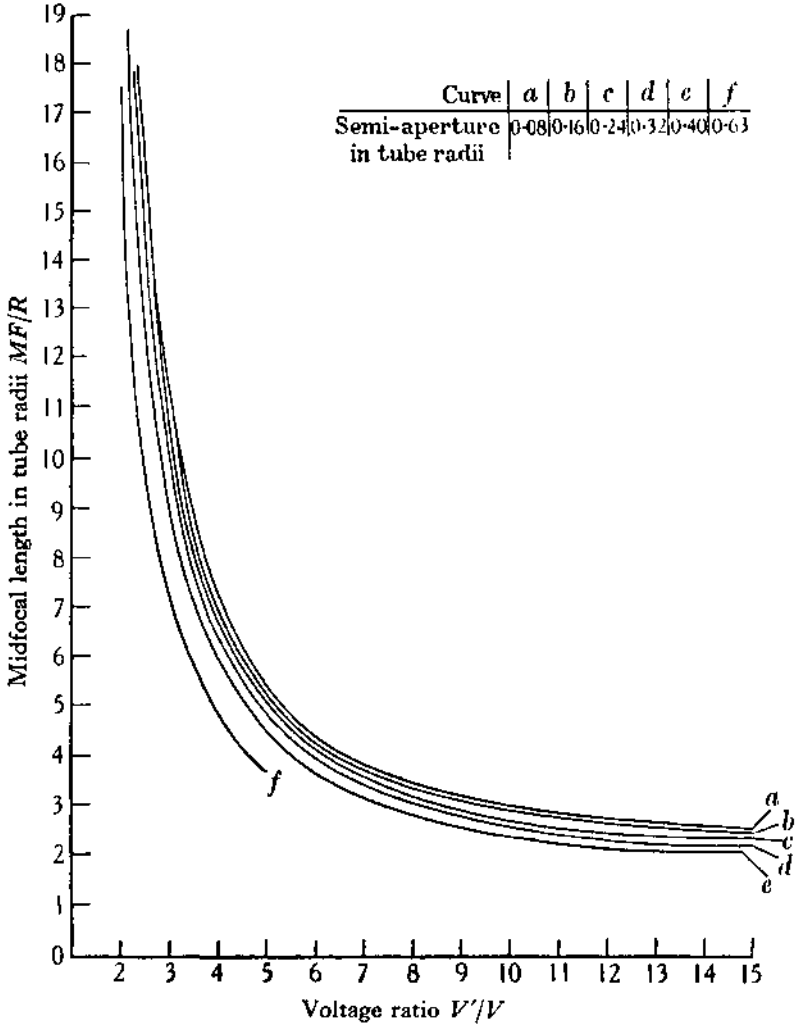

Fig. 6.2. Midfocal length as a function of voltage ratio (D.P.) for different semi-apertures.

midfocal lengths are plotted against the semiapertures of the beam. The two solid curves illustrate the spherical aberration of the symmetrical two-tube lens decelerating a parallel beam; they refer to the voltage ratios 5 and 15. The corresponding

curves for the same lens accelerating a parallel beam are plotted as broken lines. It appears that the lens is of a much better quality if the parallel beams are at the low voltage side. The spherical aberration depends to some extent on the object and image distances. The aberration for any finite object or image distance will be intermediate between the two extreme cases where object or image is at infinity. The type of estimate we have described may, however, be useful if only rough information is

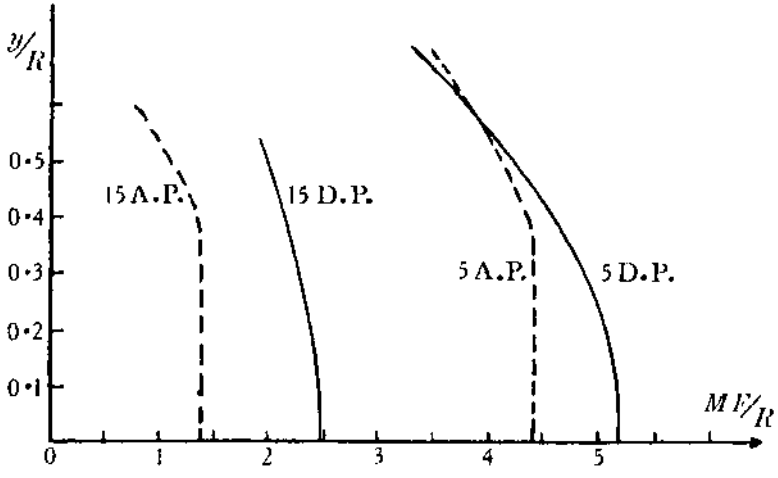

Fig. 6·3. Some spherical aberration curves for the symmetrical two-tube lens.

required; to obtain accurate results for any particular case, special measurements with the proper object and image distance have to be performed.

From aberration curves, such as those of Fig. 6-3, it appears that the spherical aberration decreases with increasing voltage ratio. It should be kept in mind that for the quality of an optical image it is the ratio of aberration to focal length that counts. However, the focal length will also decrease with increasing voltage ratio.

According to O. Klemperer and W. D. Wright (K. 3) trigonometrical ray tracing reveals for the two-tube lenses that the equipotentials close to the midplane supply relatively small

contributions to the total spherical aberration. The main contributions are produced by regions of the potential field which lie at some distance on both sides of the midplane. With a view to obtaining improved lens designs it is therefore again of some practical help to consider (as in Chapter iv) the two semilenses constituting any complete two-electrode lens. It then appears that the semilens on the low voltage side always shows positive aberration, whilst the aberration of the semilens on the high voltage side is always negative. Therefore, the question of the removal of the spherical aberration becomes a question of matching the semilens with positive aberration against the semilens with negative aberration. This can be done to some extent by changing the size and the shape of the electrodes. Definite improvement can, for instance, be obtained for a two-tube lens if the diameter of the electrode at the high-voltage side is chosen to be smaller than the diameter of the electrode at the low-voltage side (W. 2).

Magnetic lenses generally show some positive spherical aberration, especially the lenses with extremely short focal length as used for high magnification electron microscopes (Chapter vn). This aberration is considerable and largely impairs the resolving power of the microscopes. E. Ruska (R. 4) investigated some magnetic lenses, and found for apertures of only half the width of the diameter of the pole shoe employed, that marginal focal lengths were 20 to 30% shorter than the paraxial focal length. In other cases, however, if lenses with relatively long focal length can be employed, the magnetic coil may be large in comparison with the aperture actually used, and then the aberration is often negligibly small.

For practical purposes the quantitative effect of the spherical aberration on the quality of any image point is most important. In the presence of spherical aberration, a perfectly sharp focus of a wide bundle of rays becomes impossible, since every zone of the bundle produces a different focal point.

The rays of a bundle of electrons focused by a lens with spherical aberration may be received on a sliding fluorescent

target which is arranged so as to be always perpendicular to the optical axis. If the target is gradually moved along the axis, the radius of the fluorescent circle marking the cross-section of the bundle passes through a minimum at a place which is some distance from the paraxial focus *F*. This minimum diameter corresponds to the best possible focus. The disc of electrons formed at this best focus is called the disc of least confusion.

Take, for instance, the rays (2) and (4) in Fig. 6.1i, which represent the wall of a cylinder since this diagram shows an axial cross-section. This cylinder surrounds a bundle of parallel beams of electrons. As shown in Fig. 6.1, and in an enlarged scale in Fig. 6.1a, the beams are focused and reach a minimum cross-section at the point C, *CS* being the radius of the disc of least confusion. The beams passing the periphery of the disc of least confusion are focused on the axis at F_c and at F_n respectively, and they intersect the axis at the angles Θ_c and Θ_n. The spherical aberration FF_n of a beam *(n)* may be assumed to be proportional to the square* of its aperture, so that

$$FF_n = \qquad a\tan^2\Theta_n, \tag{6.1}$$

a being a proportionality factor and tan Θ_n being used here as a convenient measure of the aperture of the beam *(n)*.

The distance of the focus F_n from the centre *C* of the disc of least confusion is given by

$$\begin{aligned} CF_n &= F_cF - F_nF - F_cC \\ &= a(\tan^2\Theta_c - \tan^2\Theta_n) - x, \end{aligned} \tag{6·2}$$

if $F_cC = x$. The radius *h* of the disc of least confusion is

$$\begin{aligned} CS = h &= x\tan\Theta_c = CF_n\tan\Theta_n \\ &= [a(\tan^2\Theta_c - \tan^2\Theta_n) - x]\tan\Theta_n. \end{aligned} \tag{6·3}$$

From the third and the last terms of this equation one obtains, by adding $x\tan\Theta_n$

$$x(\tan\Theta_c + \tan\Theta_n) = a(\tan^2\Theta_c - \tan^2\Theta_n)\tan\Theta_n$$

or

$$x = a\tan\Theta_n(\tan\Theta_c - \tan\Theta_n),$$

* If the aberration is assumed to be proportional to a higher power of the aperture the result of this calculation is not much altered.

and with eq. (6.3),

$$h = a(\tan \Theta_n \tan^2 \Theta_c - \tan \Theta_c \tan^2 \Theta_n). \qquad (6{\cdot}4)$$

In order to find the maximum value of h, if Θ_n is varied, eq. (6.4) may be differentiated with respect to tan Θ_n and then put equal to zero:

$$\frac{dh}{d \tan \Theta_n} = a(\tan^2 \Theta_c - 2 \tan \Theta_c \tan \Theta_n) = 0$$

or

$$\tan \Theta_c = 2 \tan \Theta_n.$$

Putting this value in eq. (6.4), one finds

$$h_{\max} = \frac{a}{4} \tan^3 \Theta_c, \qquad (6{\cdot}5)$$

or with eq. (6·1),

$$= \frac{FF_c}{4} \tan \Theta_c. \qquad (6{\cdot}6)$$

Eq. (6.6) shows that the radius of the disc of least confusion of any focused bundle is equal to a quarter of the longitudinal spherical aberration of the beam *(c)* with the largest aperture, multiplied by the tangent of the slope angle of this beam.

In cases where the aberration of a lens is given by curves like those of Fig. 6.3, it is convenient to replace tan Θ_c of eq. (6.6) by the ratio between the extrapolated semiaperture of the bundle at the midplane, and the midimage distance. Formulated in this way, eq. (6.6) is particularly useful for the calculation of the spot size in cathode-ray tubes (see Chapter vll). There, from the aberration curves of the focusing lens, the size of the image spot can be deduced immediately as a function of the applied size of the aperture stop, provided that the electron source (i.e. the cross-over, see Chapter vll) is sufficiently small to be treated as a point object.

If points lying off the axis are reproduced by rays of large semiaperture, a lens error called coma causes an unsymmetrical deformation of the individual image points to a comet-like appearance. The coma is usually determined as the distance from the focus of the marginal pair of rays to the principal ray.

To illustrate this, in Fig. 6.4 parallel beams are shown crossing the axis at an angle *0.* If the lens were perfect, all the beams would be focused at the point *E* which lies in the plane intersecting the axis *Z* at the focus *F.* If the lens suffers from coma only, the rays close to the principal ray (1) will be focused at *E,* but rays with larger semiaperture will be focused at a different point *C* in the image plane *FE,* the zonal variation *CE* being a function of the semiaperture of the beam. On the other hand,

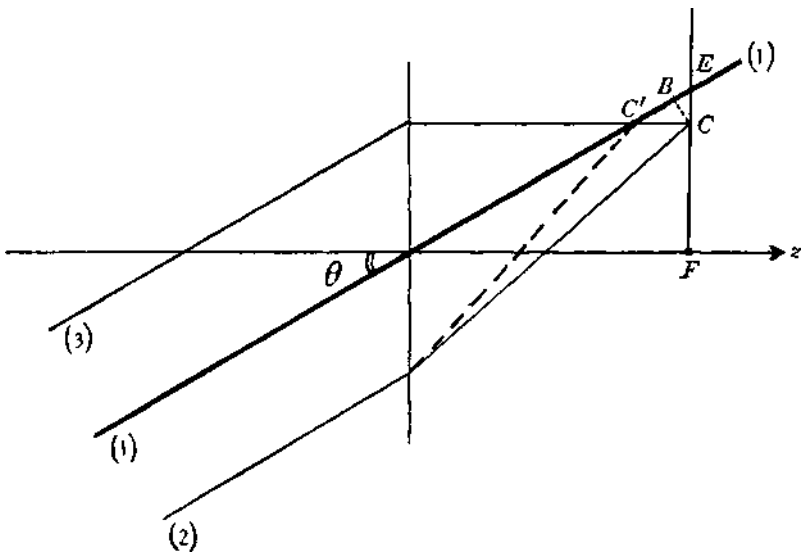

Fig. 6.4. Thin lens with coma (C) and thin lens with spherical aberration (C).

spherical aberration would cause a shift of the marginal focus along the central beam, say to a point C\ If both coma and spherical aberration were present, the intersection of the marginal beams could happen anywhere off the central beam and off the focal plane. Thus in a picture a general lack of definition would result and the blurring would increase with increasing distance from the axis.

The simplest way of stating the absence of coma is due to Abbe. In the third order theory, Lagrange's equation (2.8) has to be replaced by

$$Vy \sin \Theta = V'y' \sin 0', \qquad (67)$$

as soon as beams with wide angles are being used. This new equation is contradictory to the mathematical scheme of the collinear relationship, but it is required if we are to obtain extended, true images, and it satisfies general physical laws. Its validity can be derived from the laws of thermodynamics. From eq. (6.7) it follows that the lateral magnification y'/y should be a constant for all zones if $\sin \Theta'/\sin \Theta$ is a constant. For an infinitely distant object $\sin \&'$ is proportional to the height y of the incident beam, so that $y/\sin 0$ should be constant for incident parallel beams and should be identical with the focal length PF of the system:

$$\frac{y}{\sin \Theta} = PF. \tag{6.8}$$

In the first-order theory, parallel beams and their directions, after being focused, intersect in the principal plane. As can be seen from eq. (6.8) this is no longer true for large semiapertures. For a lens which is free from coma and spherical aberration these intersections should take place on a spherical surface, the radius of curvature of this "principal surface" being the focal length. If no other aberrations were present, the deviation of the principal surface from the spherical shape would reveal coma. In the case where the lens suffers from spherical aberration the coma could be found by subtracting the spherical aberration from the paraxial focal length along the various rays.

Although this method is interesting in principle, the measurement of the shape of the principal surfaces by experimental electron-beam tracing is generally not accurate enough to give more than rough qualitative information about the coma. For any quantitative investigation a direct tracing of the zonal variation of the axial distances of focal points as indicated by Fig. 6.4 should be preferred.

A most serious lens error in electron optics is the curvature of field. It causes the image of a plane object to be formed upon a curved surface instead of the usually desired flat image plane. When astigmatism is also present, then there will exist two

curved image surfaces, corresponding to the sagittal and the tangential foci. This may be illustrated in the following introductory manner. Take as object a wheel with its axle lying in the axis of the lens system. Then the rim of the wheel will be projected sharply on to the tangential image surface, whilst the spokes of the wheel will appear to be focused sharply in the sagittal image plane. More exact explanations may be given by means of Fig. 6.5, where z is the lens axis and (1) is the central ray of a bundle of rays crossing the axis at O. The two

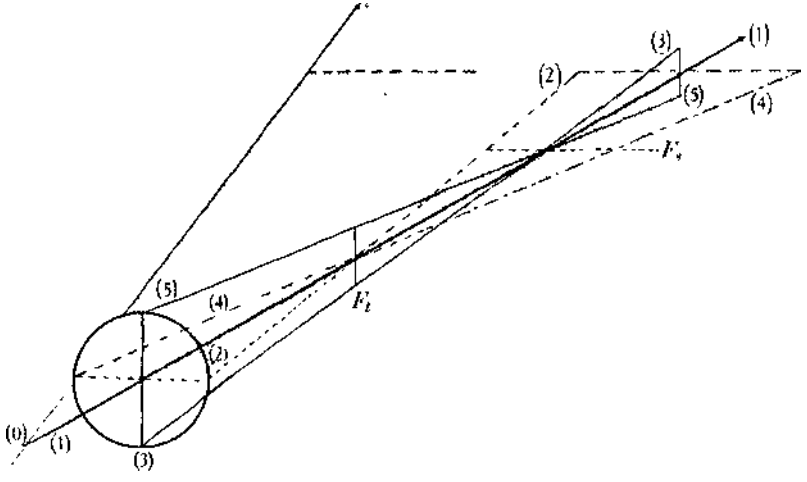

Fig. 6.5. Astigmatism of a small bundle of rays.

tangential beams (2) and (4) and the two sagittal beams (3) and (5) are also shown. These pairs of beams indicate that the whole bundle of rays has two longitudinally separated constrictions, the tangential or primary focus F_t and the sagittal or secondary focus F_s. In absence of coma the two constrictions become sharp focal lines. At no place along the central ray is there a point focus; the nearest approach to one is about midway between the two astigmatic foci, in a disc of least confusion. Field curvature is a very severe defect of all electrostatic lenses if they are used to project an image of a flat cathode. The image surface is always strongly concave towards the cathode. Using

a symmetrical two-tube lens, G. A. Morton and E. G. Romberg (M. 6) measured axial radii of curvature of only 0.044 tube radii for the tangential image surface and of 0.075 tube radii for the sagittal one. H. Johannson (J. 1) published measurements of field curvature for a two-diaphragm objective in connection with a flat cathode. Using a flat screen as image plane, the field curvature produced a bad lack of definition at the marginal regions of the picture, so that the field of view which could be used reproduced barely a tenth of the aperture of the cathode surface. The sharply reproduced part of the aperture of the cathode surface could be increased by about 50% if properly shaped diaphragms were employed.*

If the problem of correcting an electron lens has to be attacked from a general point of view, the famous Petzval theorem, which was introduced in glass optics about a hundred years ago, is of greatest importance. For electron optical purposes it has been formulated by O. Klemperer and W. D. Wright (K. 3) in a particularly convenient form.

The electrostatic field may be subdivided as indicated in Chapter in in such a way that the ratio of the square roots of subsequent equipotentials $\sqrt{V_j}/\sqrt{V_j'}$ is a constant (see eq. (3*8)). If V_n' is the voltage of the last equipotential and *rj* is the curvature of the jth equipotential, the radius of curvature *C* of the image surface is given by

$$\frac{1}{C} = \sqrt{V_n'}\left(1 - \sqrt{\frac{V_j}{V_j'}}\right)\Sigma \frac{1}{\sqrt{V_j}r_j}. \qquad (6\cdot9)$$

Take both an image field and an equipotential concave towards the cathode. Then, the value of $1/C$ and that $c1/\sqrt{V_j}r_j$ r e assumed to have the same sign if an electron passing the equipotential surface is decelerated.

The extreme difficulty of trying to flatten the field may be

* Compare the shaped diaphragm in the electron microscope of Fig. 7.4.

† In glass optics, a field curvature concave towards the object is conventionally denned to be positive. Assuming the object in air, a glass surface, however, concave towards this object, has, according to the usual conventions, a negative sign of curvature.

realised from a consideration of eq. (6.9). If, for instance, a two-tube lens is used to project the electrons from a flat cathode on to a flat screen, the electrons are accelerated in passing the equipotentials of the lens, and these are convex towards the cathode at the low potential side of the midplane (see Fig. 3.2) so long as V_j is small. It therefore follows that the first semilens will produce a large part of the sum $\Sigma \frac{1}{\sqrt{V_j} r_j}$. However, when the curvature of the equipotential has changed sign (in the second semilens), the electrons have already gained so much velocity that there are only a few equipotentials with opposite sign

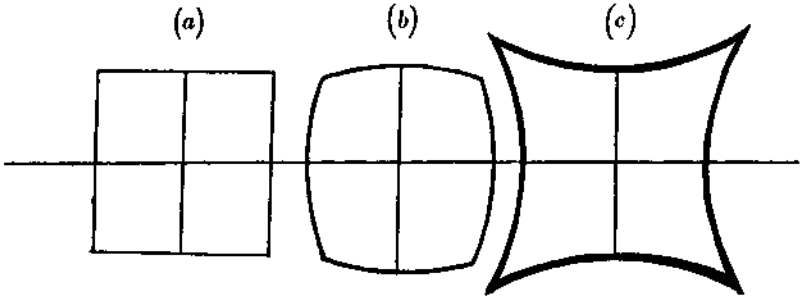

Fig. 6.6. *(a)* Object. *(b)* Barrel distortion. *(c)* Pincushion distortion.

contributing to the sum in eq. (6.9), and V_j is so large that the terms $1/\sqrt{V_j} r_j$ are small. Hence 1/C will be a large sum giving C as a small radius corresponding to a steeply rounded field concave towards the cathode.

As the fifth isotropic error we discuss the distortion. This is somewhat different from the other four errors, as it has no effect upon the sharpness of the individual image points; it merely displaces them towards or away from the optical axis. The magnification in the central part of the image is fixed by Lagrange's law (eq. 2.8), thus the distortion can be measured by the distance from the actual marginal image point to its ideal position as determined by Lagrange's law. If the ideal image point falls above the actual one, the outer parts of the image are on too

small a scale and the distortion is called "barrel distortion" (see Fig. 6.66). If the outer parts are on too large a scale, "pincushion distortion" will occur, as illustrated by Fig. *6.6c*. Electron lenses generally show pincushion distortion (Z. 2), an electron mirror may produce either kind of distortion according to the special conditions (N. 1).

Magnetic electron lenses also show the five isotropic errors which we have just discussed for the electrostatic lenses. There are also three anisotropic errors which deteriorate the quality

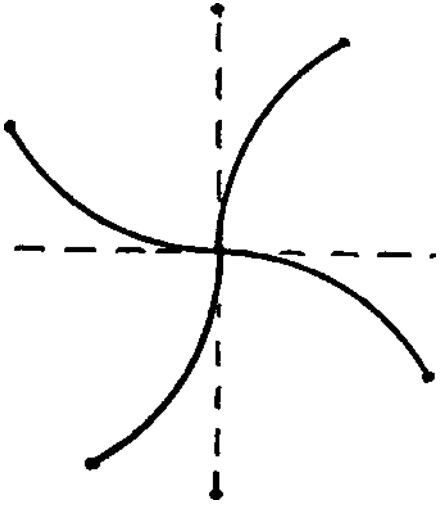

Fig. 6.7. Spiral distortion.

of the images produced by magnetic lenses. Although these three additional errors are possible in the case of magnetic lenses, the general impression seems to be that the images produced by simple uncorrected magnetic systems are generally of a better quality than those produced by primitive uncorrected electrostatic lenses.

The anisotropic distortion of a magnetic lens, often called the spiralling distortion, is an error which is caused by a rotation of the image (eq. (5.19)), which is not perfectly proportional to the radial distance of the image point. In Fig. 6-7 are indicated two broken, perpendicular lines forming a cross, which may be scratched on

the cathode as the object of the system. The spiral shape of the corresponding image is drawn in the same figure as two solid lines. The marginal rotation is generally larger than the axial one; thus it seems possible to improve this error by decreasing the strength of the marginal part of the magnetic field.

Anisotropic coma occurs when not only the whole image is rotated round the axis of the lens, but any single element of the picture is also rotated round its proper centre. There results an unsymmetrical deformation of the individual image points to a comet-like apperance. The tail of the comet is not, however, radially directed, as with isotropic coma, but lies in a direction perpendicular to the radial co-ordinate.

The last error is anisotropic astigmatism.* This error causes a marginal object point to be projected in a line focus which is inclined at an angle of $\pi/4$ to the radial co-ordinate. The image surface where these line foci are sharp, is generally curved. Therefore in the image plane a general confusion will result, especially in the marginal zones.

The theory of the anisotropic errors of magnetic lenses has been worked out very thoroughly by W. Glaser (G. 2). On the experimental side only a few qualitative investigations have been published. K. Diels and G. Wendt (D. 3) demonstrated the existence of all the eight third-order errors in a magnetic lens by investigating the image of an electron point source.

The Hartmann test, which was explained at the beginning of this chapter in the discussion of spherical aberration, has not yet been used to trace the field errors of electron lenses. Since it is common practice to employ this test for the measurement of all lens errors in glass optics, a few words may be said in illustrating the possibility of its application for measuring field errors of electron lenses. The pepperpot diaphragm producing the fine electron pencils has its holes arranged in a straight row and the lens axis is inclined with respect to the central electron beam. Fig. 6-8 shows an arrangement where the series of beams (o), (2), (4) lie in the same plane as the axis z of a lens system

* This is called anisotropic spherical aberration by some authors.

indicated by the square L. Comparing Fig. 6-8 with the perspective drawing of Fig. 6-5, it is obvious that tangential lens errors may be measured by the arrangement of Fig. 6-8. The two beams (3) and (5) of Fig. 6,5 lying in a plane perpendicular to the beams (2) and (4) could be produced by turning the pepperpot diaphragm through 90^0 round the central beam. In Fig. 6-8, the beams (2) and (4) cross over at a point *C*. According to the explanations given earlier in this chapter, the coma is measured by the distance *CB*, *B* being the intersection of the perpendicular from *C* on the central ray (O). The perpendicular

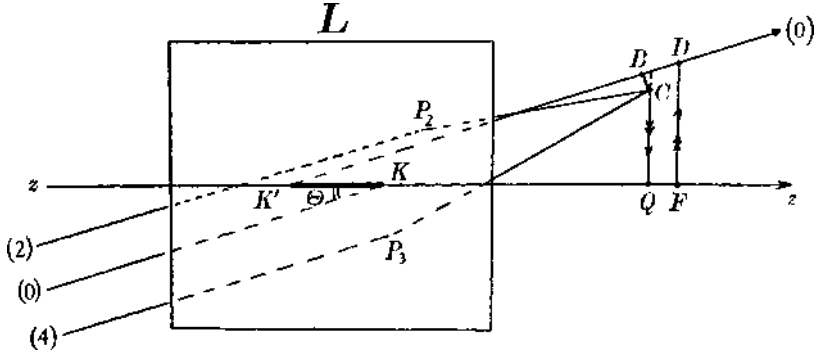

Fig. 6.8. Measurement of tangential lens errors.

from *C* on the lens axis *z* intersects the latter at *Q*. If *F* is the paraxial focus, the distance *QF* will measure the field curvature. If a perpendicular to the z-axis through *F* intersects the central beam at D, the distance *FD* may be taken to measure the distortion. None of the beams seems to pass straight through the thick lens system. The central ray (O) of Fig. 6-8 is a "nodal" ray; it can be recognised, since it enters and leaves the lens with the same direction. Its prolongation has to intersect the lens axis at the nodal points *K* and *K'*.

All the other errors could be investigated in a manner similar to that described for the measurement of the four tangential isotropic field errors, and illustrated by Fig. 6-8. Their diagrammatic representation would, however, not be so simple

as Fig. 6,8, because generally the intersection of the beams would not occur in the plane which is defined by the original series of parallel pencils. We must refrain here from going more into detail. The electron optical research of the next few years will have to pass through a laborious phase similar to that which occurred with glass optics. The way of progress will lie in the direction of analysing lens errors and of designing lens systems as free as possible from all those errors which are found most disturbing in practice.

Chapter VII

SOME PRACTICAL APPLICATIONS OF ELECTRON OPTICS

Electron optics would never have received the attention it has, if it had been of academic interest only. It is of course beyond the scope of this tract to give a detailed review of the wide field of electron optical applications. We have to refrain here from describing all possible applications of electron optical methods to any apparatus where electrons or positive ions are being accelerated, deflected or focused. We may just mention that electron optics has shown or will show ways for the development of valves, of cathode ray,-ray, or atomic spectrographs, of electron diffraction apparatus, of X-ray tubes and of other devices. We will deal here only with the most important practical applications of electron optics, explaining the principles of the electron gun, the electron microscope, the picture transformer and the electron multiplier.

In the gun, the electrons starting from a cathode are focused into a very small image or spot. Primitive electron guns were already used in F. Braun's cathodeAray tubes in 1897. In these, however, the electrons were liberated and concentrated by means of a gas discharge. The most important: advances in gun con-struction struction were made when E. Wiechert introduced the magnetic concentration coil in 1899, and when A. Wehnelt invented the oxide cathode in 1903 and when he recommended the use oF an electrostatic concentrating electrode, the "Wehnelt-cylinder", in 1908. The first example of a modern electron gun was presented in 1933 by V. K. Zworykin (Z. 1). The general scheme of this gun is shown in Fig. 7-1. Electrons are emitted by the cathode *Ca,* they are accelerated by a first anode *A* and focused at some distance on to a fluorescent screen by means of the lens formed between *A* and a second anode Z. The intensity of the beam can be modulated by means of a diaphragm-electrode, the

so-called "grid" *G* to which a variable bias, slightly negative relative to cathode potential, may be applied. In Zworykin's gun, the spot is not the optical image of the cathode surface but of a "cross-over" of the beams which occurs close in front of the cathode. The cross-over corresponds optically to the pupil of the system. If the cardinal points of the lens between *A* and *Z* are known, the magnification $y'\backslash y$ (= the ratio of the spot radius to the radius of the cross-section of the beam at the cross-over part) is fixed for a given object and image distance.

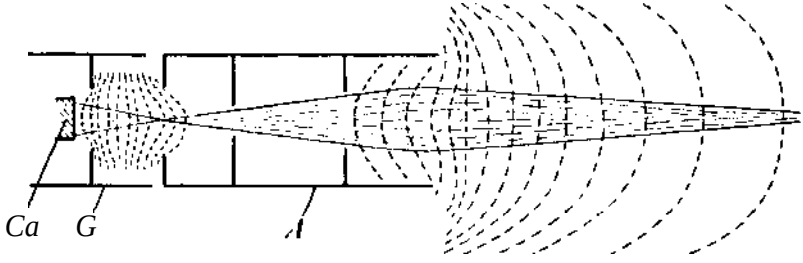

Fig. 7,i. Electron gun.

The size of the cross-over area has been discussed theoretically in a fundamental paper by E. Ruska (R. 3). Assuming a field with strictly spherical and concentric equipotentials, all electrons starting with no velocity at one of the outer equipotentials would be focused in the centre to an infinitely small cross-over. Actually the electrons have the thermal emission velocity of V_{em} equivalent volts. They leave the cathode surface at all angles. Under these conditions the calculation of the electron trajectories gives the demagnification

$$\text{Jo"} \qquad \sin 20 \qquad (7\text{-i})$$

where y_0 is the semiaperture of the emitting cathode, V_a the final voltage of the electrons and *0* the semivertical angle of the cone

of electron beams. For instance, with an emission velocity of $V_{em} = 0{\cdot}1$ volt with a final velocity of 160 volts and with a semi-aperture $\Theta = 15°$, a demagnification of I / I O would be calculated.

It can be seen that for a given density of emission, and using a given focusing lens, certain theoretical limitations for the current density i in the spot may be expected. D. B. Langmuir (L. 2) has discussed this problem, and he finds that if a Maxwellian distribution for the emission velocities is assumed, the maximum current density obtainable in the focused spot is given by

$$i_{max} = i_{cath}\left(\frac{V'e}{kT} + 1\right)\sin^2\Theta', \qquad (7\text{-}2)$$

and is limited by the cathode current density i_{cath} the absolute temperature of the cathode T\ the final voltage V and the semi-angle Θ' subtended by the beam at the final spot. Here e and k are the electronic charge and Boltzmann's constant, so that $e/k = 11{,}600$ degrees per volt. To illustrate this important conclusion we quote with a few slight alterations a table given by Langmuir:

TABLE 7-1

Theoretical maximum current density in focused spot of cathode rays

Final voltage = V'. Half angle subtended by beam = Θ'.
Cathode temperature = 1160° K. Cathode current density = 0·1 amp./cm.²

V' volts	sin Θ'		
	0·01	0·032	0·10
100	0·01 amp./cm.²	0·1 amp./cm.²	1·0 amp./cm.²
1,000	0·1	1·0	10
10,000	1·0	10	100

The major points of attack upon the problem of producing more intense electron beams are therefore indicated; namely, the final voltage has to be increased as much as possible, cathode surfaces have to be developed from which higher current densities can be drawn and focusing lenses have to be designed which are able to handle beams of wider angle without aberration.

Nothing could raise the current density above the value defined by eq. (7'2).

The actual value of the current density in the spot generally lies below this theoretical maximum for two reasons. First, for wide apertures it will hardly be possible to correct the whole system completely with respect to spherical aberration. Secondly, the mutual repulsion of the electrons can no longer be neglected in beams with exceedingly high current densities. It appears to be particularly difficult to keep a large number of electrons together in a small volume, because the Coulomb forces repelling the charges of equal sign increase with the inverse square of the distances between the electrons. If the electrons are moving, these repelling forces are partially compensated by magnetic forces producing a mutual attraction. The cause of this is the same as that which makes two electric currents flowing in the same direction attract each other. However, the repulsions overbalance the attractions in all cases, especially if the electrons are slow. E. E. Watson (W. 1) and A. Bouwers (B. 4) worked out the theory of mutual repulsion and derived in this connection formulae for the spreading of initially parallel beams. The practically important problem of the mutual repulsion of electrons focused on to a spot has received some attention in a paper by L. H. Bedford (B. 1). However, neither theoretical nor experimental investigations have yet reached satisfactory conclusions on this important problem.

Stimulated by the need for efficient television tubes, there has been a considerable development of the electron gun in recent years and the modern constructions are considerably better than the primitive example shown in Fig. 7'1. We mention in this connection the guns produced by P. T. Farnsworth (F. 1), by I. Shoenberg, G. E. Condliffe and W. F. Tedham (S. 4) and by R. R. Law (L. 3).

The performance of a recent type of high-current gun developed by the Research Laboratory of Electric and Musical Industries for use in television projection tubes furnishes an example of modern gun efficiency. Details of the design have

not yet been published, but in the commercially available E.M.I, projection receiver currents exceeding one milliamp are concentrated into a spot of less than I/IO mm. radius. In this type of receiver television pictures of great brightness are produced on a very small fluorescent screen and projected optically on to a projection screen having nearly ioo times the area of the original picture.

Whilst in common gun constructions it is attempted to obtain large currents in relatively narrow beams, there has been put forward quite a different aim in certain types of measuring gun where the generation of very wide parallel beams of homogeneous intensity over a large cross-section is required. In Fig. 7'2 we show an example of a gun which has been used by

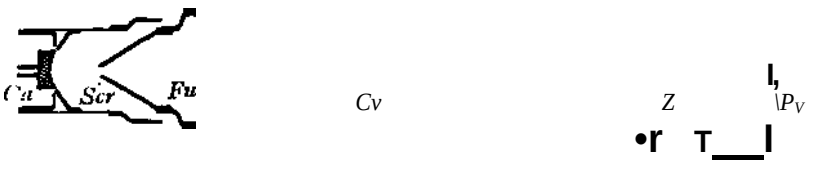

Fig. 7-2. Electron gun for parallel beams.

O. Klemperer and W. D. Wright (K. 3) and which is very well adapted for investigations of electron lenses such as were described in Chapters 11 and vi in connection with Figs. 2'1, 6-i and 6-8. In Fig. 7-2, electrons, emitted from the concave cathode *Ca,* are focused through the aperture of a funnel-electrode *Fu.* An electron lens between *Fu* and a converging electrode *Cv* reduces the divergence of the beam and another lens between *Cv* and the final electrode *Z* concentrates the beam further, so that the electrons leaiving *Z* are parallel. *Z* carries a pepperpot-like diaphragm P_p which is shown in outline in Fig. 7-3. P_p contains a line of fine holes cutting out a series of fine pencils. All but one pair of holes, which are equidistant from the axis, are covered up at a time by a movable flap *Fl,* which can be rotated round the axis *Rd* by means of a ground

joint. To produce parallel beams, the voltage ratio between *Fu* and *Cv* is about 1:5; that between *Cv* and *Z* is about 1:3 or alternatively 3:1. The absolute voltage at *Fu* can be varied over a wide range, so that parallel beams may be produced leaving *Z* with any required voltage. Since the gun cannot be made free of aberration, it is necessary, in order to produce a strictly parallel beam, to adjust slightly the voltage ratio between *Cv* and *Z* to correspond to the aperture of the pair of pencils which is going to be employed. If the electrodes *Cv* and *Z* are omitted

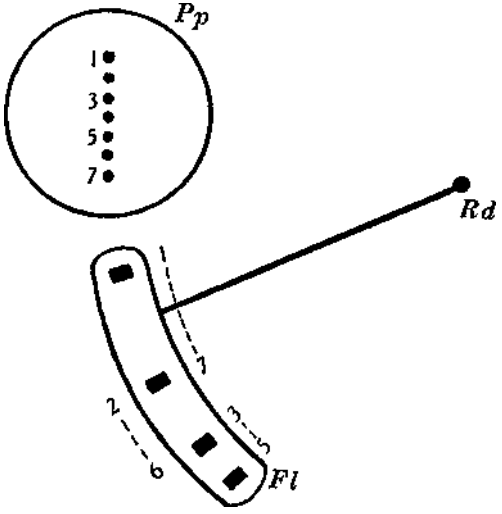

Fig. 7'3. Pepperpot diaphragm and flap.

and the pepperpot diaphragm is fixed immediately at the end of the funnel electrode, a point source can be obtained free from aberration and pencils of different divergences emerge from the holes of the pepperpot diaphragm. Such a point source proves to be very useful for lens investigations which have to be made with given object and image distances.

We next describe another group of electron optical devices which are used to form an image of an electron emitting surface in such a way that variations in current density from point to point of this surface are reproduced in the image. To this group

belongs the electron microscope. M. Knoll and E. Ruska (K. 5) in 1931 obtained high magnifications for the first time with the aid of magnetic lenses, whilst E. B ruche and H. Johannson (B. 7) succeeded about the same time in developing electrostatic microscopes. The "immersion objective" of the electrostatic microscope consists of two charged diaphragms containing circular apertures. By using the right geometrical dimensions, the focal length of these objectives can be made as short as 1 mm. Thus the projection of the electron image on to a fluorescent screen at a distance of say 30 to 60 cm., and with an object distance of little more than a millimetre, may produce a magnification of several hundred times. The shortest focal length which can be obtained with a magnetic lens is of the order of a few millimetres, so that, in this case, in order to obtain a magnification of several hundred times, either a relatively long instrument, or a magnification in two stages, has to be used.

Whether magnetic or electrostatic lenses are employed in electron microscopy will depend mainly on the sort of object which is to be inspected. The inspection of hot cathodes which are emitting slow electrons has been carried out with electrostatic objectives which are used at the same time to accelerate the electrons towards the fluorescent screen. On the other hand, if fine transparent objects, as for instance organic cells, are to be investigated, electrons of high speed have to be transmitted through the object. In this case only powerful magnetic lenses are able to project an image of these fast electrons on the screen.

An interesting instrument which allows the comparison of microscopic pictures produced by light with those produced by magnetic lenses or by electrostatic lenses has been described by W. Knecht (K. 4). It is shown in Fig. 7-4. There, *K* represents the thermionic cathode used as the object emitting electrons which are accelerated by the diaphragm-anode *A*. The cathode is connected to earth and the anode, together with the cylinders Z, is charged positively to about 700 volte. The shaped electrode *G* between *A* and *K* is at a variable potential, which is only slightly different from cathode potential, and

which has to be adjusted according to the distance between *K* and *G* (object distance) controlling the magnification of the image which is projected on to the fluorescent screen *S*. The object distance can be changed by adjusting screws stretching the flexible copper bellows *R*. By means of a large ground joint the cathode system can be removed from the tube and thus the object can be easily changed. For a magnetic projection, both electrodes *G* and *A* are at common anode potential. The iron-shielded magnetic coil *M* is energised by an electric current and projects the magnified image directly on to the screen *S*.

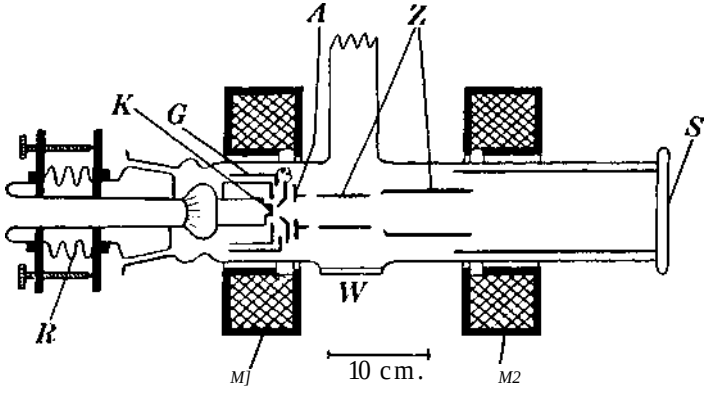

Fig. 74. Combined electron microscope.

The power of *M* may be chosen large enough to produce an intermediate image inside the cylinder Z. This imagne can be magnified again when it is projected on to the screen by means of a second magnetic lens M_2. In a different kind of operation electric and magnetic lenses can be employed together. Such a superposition of electric and magnetic fields is very useful from the practical point of view, because it allows different magnifications without the necessity for moving the object.

If microscopic observations have to be made by means of ordinary light, the electrode system *G*.. .*A* and the cylinders *Z* can be removed by a ground joint (not shown in the figure) and a glass objective can be put in its place. A rectangular prism

fixed on top of this glass objective allows visual observations to be made through the window *W*. [See also (M. 3).]

The only noticeable difference between the images produced by the electric and magnetic lenses was that the latter produced a better definition at the margin of the picture, probably because this type of lens suffers to a smaller extent from field curvature. The images formed by the light microscope and the electron microscope were geometrically similar, but might show appreciable differences in the details. Peculiarities due to changes in electron emission are visible in the electron picture but not in the light picture. For instance, the electron microscope is able to detect the crystal structure of a nickel cathode on top of which a thin barium layer is sprayed. It then appears that the Richardson work function of the barium layer is changed in different amounts by the different crystal faces underneath it.

By inspection of electron pictures of this kind it was possible to obtain new information about the mechanism of thermionic emission, and in particular the activation process of oxide cathodes and of thoriated tungsten filaments could be cleared up in essential points (B. 11, H. 3). Moreover, the possibility of an electron optical investigation of metal surfaces has opened up a new field of metallographic research. Electron optical patterns corresponding to a crystalline texture are suitable, for instance, for the observation on transition of iron from the *a*- into the y-modification(B.g, B. 12). The bottom figure on the frontispiece shows an electron optical picture of this kind which was taken by W. G. Burgers and J. P. van Amstel (B. 12). In this particular experiment the cathode was made from a tapered iron strip activated with Sr and Ba. As the tapered cathode varied in its electrical resistance from place to place, a temperature gradient occurred along the strip. At the wider side of the strip, the temperature was below the transition temperature (about 900^0 C.) and the iron showed there the cubic body-centred a-modification. At the narrower side of the strip, the temperature above the transition point and the cubic face-centred -y-modification was apparent. The boundary line between the two modifications,

which is clearly visible in the photograph, is marked by an arrow. By either increasing or decreasing the cathode heating current, the position of the boundary, where the transition temperature occurred, could be shifted. In this way it was possible to observe and to record the growing of the a- or of the y-crystallites.

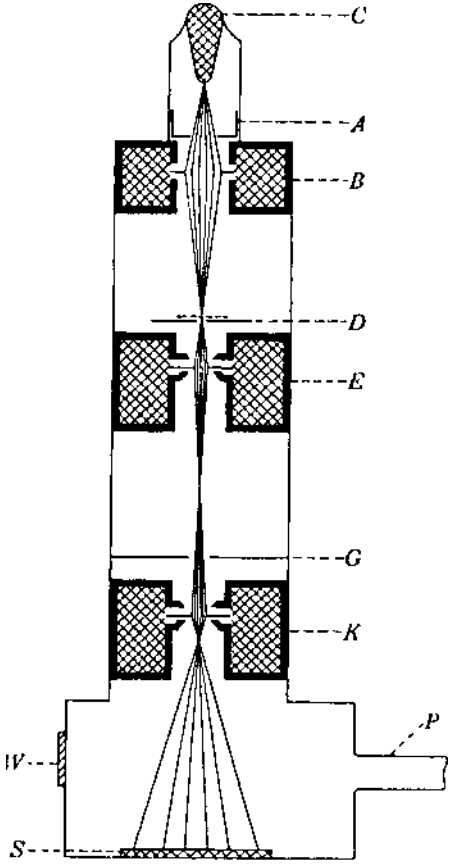

Fig. 7.5. Magnetic electron microscope for very large magnifications.

To add a few more examples it may be mentioned that successful investigations in this direction have been performed on the surface of nickel (B. 8) and of tungsten (B. io).

The above investigations have all been done with hot, self-emitting cathodes. A different microscopic technique is needed for the investigation of small objects inspected by transmitted

rays of high velocity electrons. To explain the latter method, we show in Fig. 7-5 the scheme of Knoll and Ruska's magnetic microscope. Electrons are liberated from a cathode *C* by a low-pressure gas discharge and are accelerated through an anode diaphragm *A* to a final velocity of the order of 60 kilovolts. The electrons are concentrated by the condenser coil *B* on to the object lying in the plane *D*. The objective coil *E* forms in the plane G, an intermediate electron image, which is projected on to the fluorescent screen *S* by means of the projection coil *K*. The screen can be observed through the viewing window *W*. The whole arrangement is evacuated by continuous pumping through the tube P. The iron pole pieces of the coils project into the vacuum in order to make the magnetic fields as strong as possible. In this way focal lengths of the order of 0-5 cm. can be obtained, and, with a distance of 60 cm. between the plane of the object *D* and the screen *S*, magnifications of several thousand times may be obtained with this two-stage instrument. At these large magnifications the electron density at the screen is of the order of 10^7 times smaller than it is at the object, and although the fluorescent screens are very sensitive at these high electron velocities, the light emission is very weak. Therefore the initial electron density has to be as strong as the object can stand without being destroyed.

The great merit of electron microscopes of this kind is their high resolving power. According to Abbe, the smallest distance *d* which can be resolved by a microscope is given by

$$d = \lambda / N \sin \epsilon, \tag{7-3}$$

A being the wave-length of the rays producing the picture and $N \sin e$ being the numerical aperture of the microscope. The wave-length of light $(\approx 10^{-4}-10^{-5}$ cm.) is about 10^5 times larger than the de Broglie wave-length* of 60 kilovolt-electrons

. The de Broglie wave-length of the electron, measured in A.U. (= 10^{-8} cm.) is

$$\lambda = \frac{12{\cdot}2}{\sqrt{V_{\text{volt}}}} \frac{1}{\sqrt{1 + 9{\cdot}8 \times 10^{-7}\, V_{\text{volt}}}}.$$

An extensive table of A as a function of the voltage can be found in K. 1, p. 01.

(5×10^{-10} cm.). The numerical aperture of the electron microscope of Fig. 7-5 may be estimated to be of the order of 0-02. The resolving power of this microscope would, however, not be expected to be as high as the value 10^{-8} cm. calculated with eq. (7'3)- M. v. Ardenne (A. 1), in a careful discussion of all facts which might deteriorate the definition of the microscopic image, comes to the conclusion that present-day electron microscopes of the most efficient construction using 50 kilovolt-electrons would not be able to resolve smaller distances than about 10^{-7} cm. Besides (1) the error due to the diffraction of the electron wave and (2) that due to spherical aberration, there have to be considered:

(3) Errors due to mutual repulsion of the electrons, which occur because the current density at the object has to be extremely high in order to obtain an exposure time of the order of seconds.

(4) Errors due to fluctuations of the magnetic field. (For instance fluctuations of 10^{-5} Gauss would reduce the limit of resolving power to 10^{-6} cm.)

(5) Chromatic aberrations due to fluctuations of the accelerating voltage.

(6) Chromatic aberrations due to the straggling of electron velocities In the object (band width of losses of velocity of electrons passing material sheets).

(7) Errors due to the scattering of the electrons at the object.

(8) Errors due to spurious magnetic fields, especially stray fields.

If the combined effect of all these errors is taken into account, the above-mentioned lower limit of 10^{-7} cm. is obtained for the resolving power.

The actual experimental results seem to support this estimate. Exact measurements of these extreme resolving powers have not, however, yet been made, as it is not possible to obtain suitable, test objects. The smallest distance which has been actually resolved by an ultraviolet light microscope is 10^{-5} cm., the smallest distance which can be distinguished in the electron

microscopic pictures obtained by F. Krause (K. 7, A. 1) is at least ten times smaller. There a resolving power of 4×10^{-7} cm. was revealed, corresponding to the finest structures which were available for objects suitable for electron microscopy.

Test objects in this case were the skeletons of diatoms (microscopic water algae), which were fixed on a molybdenum wire gauze. An electron microscopic picture of some of these diatoms *(Amphipleura pellucida)* which has been taken by F. Krause (K. 8) is shown in the top figure of the frontispiece. The magnification is about 3500 times. The high resolution may be judged by looking at the fine structure in the right upper part of the picture. Diatom cells are very suitable for electron microscopy, since they are strong enough to stand the electron bombardment produced by the intense beams which have to be transmitted through the object in order to produce an image of sufficient intensity. However, with proper precautions electron microscopic inspection of much more fragile objects has been successful, for instance, the fine hairs on the wing of a fly could be made visible (D. 5). Moreover, the nuclei of certain epithelium cells have been reproduced without any special preparation of the object (B. 14). Recently, even bacteria and spores of pathogenic organisms were observed (K. 8, B. 3).

A special technique of preparation of organic objects has been introduced by L. Marton (M. 5), who soaked the organic cells with osmium salts. Thus after the organic substance was burned away by the electron bombardment, the remaining osmium skeleton revealed the cell structure in a beautiful manner.

Instead of transmitting electrons through the object, other procedures have sometimes been found suitable for "illuminating' ' the object. For instance, photoelectrons liberated by visible or ultraviolet light or by X-rays, primary electrons reflected at the object surface, and secondary electrons released at this surface, have been used successfully to form magnified electron images on the fluorescent screen. However, these latter methods have not brought particularly new information nor have they been developed to the same extent as the microscopy

with thermionic cathodes and that with high-speed electrons transmitted through the object.

Electron miscroscopy is to-day in a preliminary stage. There are still large possibilities of correcting the microscopic systems or of using quite new lens or mirror arrangements with a view to improving the instrument itself. Moreover, the technique of preparing the object and of " illuminating'' it is still comparatively undeveloped, so that there is every hope for important developments of this new electron optical device in the future.

For practical purposes it is not only of interest to project highly magnified images; it is often useful to project images which are roughly equal in size to the electron-emitting object. This type of projection is used in the so-called " picture transformer''. In this instrument a light image is projected by means of a glass lens on to a photoelectric layer. This layer emits electrons which are focused on to a target by means of electron lenses. If the target is a fluorescent screen the picture transformer may be used, for instance, to transform an image formed by infra-red rays which liberate the electrons from the photoelectric layer, into a picture of visible light which can be observed directly on the fluorescent screen (S. 2). In another application the target is the mosaic of an iconoscope, the resulting instrument being the very sensitive projection emitron which has been used successfully in modern television (L. 4, M. 4).

The simplest type of picture transformer would consist of a plane transparent photocathode, a plane fluorescent screen and an ordinary two-tube lens between them, accelerating and projecting the electron image from the cathode to the screen. Such an arrangement, however, suffers so badly from field curvature and from distortion (see Chapter vi) that it is practically useless.

A great improvement oyer this simple electrostatic arrangement was obtained by the arrangement of V. K. Zworykin and G. A. Morton (Z. 2, M. 6), which is shown in Fig. 7'6. There the photocathode is slightly curved (radius of curvature about two tube radii). In this way the field curvature of the image is cured

to a large extent because the marginal parts of the cathode have a decreased "object distance", so that the marginal parts of the image have an increased "image distance". The pincushion distortion of the image is also eliminated by the curvature of the cathode, since the electrons are accelerated from the start towards the axis and therefore the uncorrected marginal parts of the electron lens are avoided. The electrons are accelerated by a chain of short lens tubes (1) to (6) which are kept at given potentials by a potentiometer arrangement so as to produce the best obtainable potential distribution. The electrons then pass a diaphragm (7), the potential of which controls, to a certain

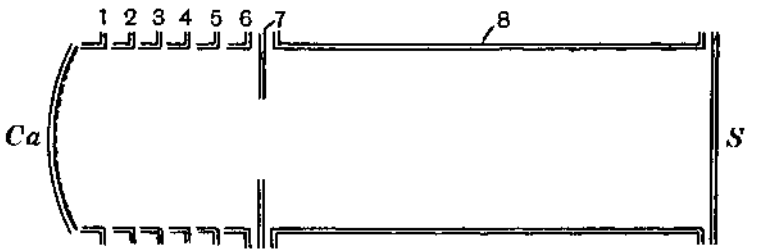

Fig. 76. Electrostatic picture transformer.

extent, the magnification of the picture. By the further accelerating electrode (8) the electron picture is projected on to the fluorescent screen *S*.

Although pictures of good quality are obtained by the arrangement of Fig. 7-6, the curvature of the cathode is very awkward, since the commercial glass optical systems which are available for projecting the light image on to it produce images with flat fields. Therefore the transformer can only be used with optical lenses of relatively small apertures providing images with sufficient depth of focus.

Image transformers with flat cathodes can only be operated with the aid of magnetic lenses. Suitable arrangements of this kind have been designed by W. Heimann (H. 2) and by I. D. McGee and G. Lubszynski (M. 4). The scheme used by the latter authors is shown in Fig. 77. The flat cathode *C* is sur-

rounded by a guard ring which curves the equipotentials in such a way that the emitted electrons are accelerated from the beginning towards the axis. The cylindrical tube *T* and the target *S* are at a common positive potential. A magnetic field produced by the iron-clad coil *M* is superimposed over the whole arrangement.

As an alternative to the short coil P. T. Farnsworth (F. i) has projected electron images by means of long, substantially

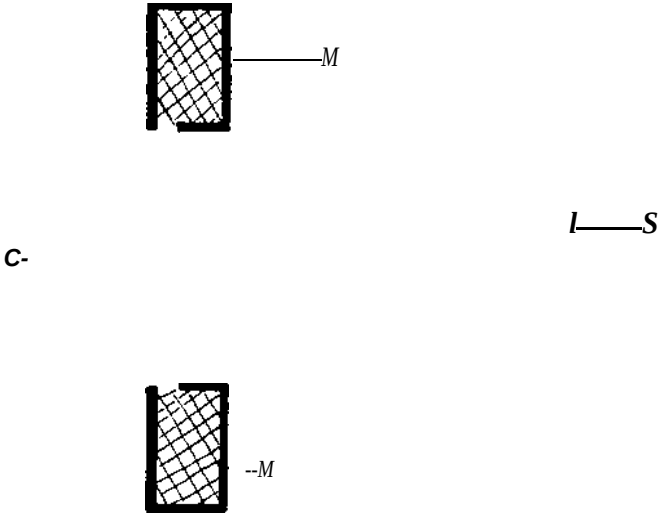

Fig. 7-7. Electrostatic magnetic picture transformer.

homogeneous magnetic fields. In his arrangement, strictly homogeneous electric fields are necessary to accelerate the electrons. The combined homogeneous electric and magnetic field is suitable for projecting an image of good quality. The desired electric field can be produced by a very thin metallic layer of high resistance producing a cylindrical electrode along which a linear potential gradient is maintained.

The lens errors which were discussed in Chapter vi are not the only factors limiting the definition of the images in picture transformers. The initial velocities of the electrons are generally large enough in comparison with the final velocity to produce

an aberration analogous to the chromatic error in light optics. W. Henneberg and A. Recknagel (H. 4) calculated for systems such as those shown in Fig. 7-7 the radius r of the disc of least confusion due to the chromatic aberration. It is given by

L being the distance between cathode and target, $y'\backslash y$ the magnification, $A\,V$ the width of the energy band of initial emission velocities and V the final velocities of the electrons. For instance, suppose L is 20 cm. and the electrons from a photocathode having a velocity distribution with the most probable value of 1 volt are accelerated to 500 volts and projected with unit magnification. Then the mean radius of the circle of least confusion, r = o'4 mm., would be expected. Of course r would become much smaller if higher final velocities could be used, but generally the values of V are restricted for practical reasons.

A further interesting application of electron optics is found in secondary emission multipliers. When certain surfaces are bombarded by cathode rays, they emit secondary electrons, the number of which depends on the material which is bombarded and is a function of the primary electron velocity. Specially prepared composite surfaces, such as caesiated silver oxide, have a maximum ratio of 8 to 10 secondaries per primary electron. This maximum occurs at bombarding potentials between 400 and 600 volts. During the past fifteen years it has become recognised that secondary emission could be used as a means of amplifying a small initial electron current. The idea suggested was to direct the initial electron current upon a target which was sensitised for secondary emission. The secondary emission from this target would be directed upon a second target which produced still further electrons, and in this way the multiplication would be repeated any desired number of times. It is interesting to state that the early schemes of multipliers gave very poor results and that the first efficient models were only produced

recently when the development of electron optics provided the basis for a suitable design. In Fig. 7-8, there is shown a simple multiplier working with electrostatic electron lenses (Z. 2, Z. 3). Electrons leaving an emitter *C* are projected by the accelerating two-tube lens L_t on to the sensitized target T_1 where secondary electrons are liberated. These secondaries are accelerated and focused by the two-tube lens L_2 on to the target T_2, where they are again multiplied by secondary emission. By the lens L_3 the electrons can be projected to a further stage, and so on. As the

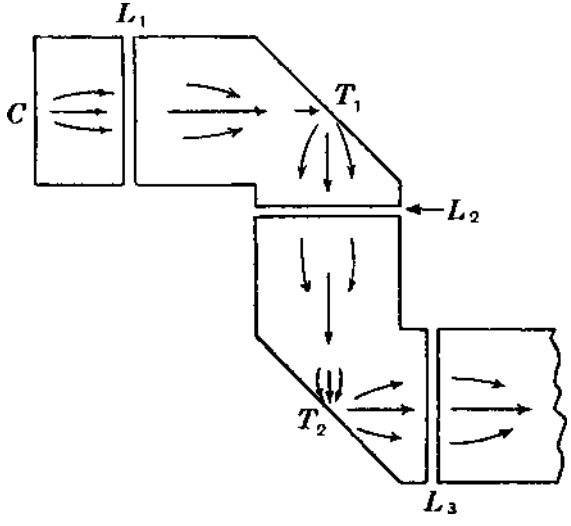

Fig. 78. Electrostatic multiplier.

secondary electrons leave the target with relatively small velocities, the voltage ratio of the lenses L_1 L_2, L_3, etc. is nearly infinite, so that, over a wide range, the magnification is found to be given by $q/2p$, p and q being midobject and midimage distance respectively. It is convenient to focus the electrons at the centres of the targets T_1 T_2, T_3, ... with about equal spot sizes; for that reason the lengths of the two tubes of the projecting lenses L_1, L_2, L_3, ... are chosen to be equal to about 4/3 and 8/3 tube radii respectively. The emitting spot on the initial cathode has to be kept small if an accurate focus is to be maintained. The

multiplier therefore becomes space-charge limited at rather small current values, since the field at each target drawing away the secondary electrons is rather weak.

This limitation, however, does not seem to be fundamental, as some other types of multipliers are not appreciably affected by space charges. In particular, a magnetic-electric multiplier with cylindrically symmetrical fields, which will be described later on (Appendix), has been used with many stages for extremely high amplifications.

Considering the successful operation of electron multipliers, the possibility of projecting electron optical images on to multiplying targets in order to obtain amplified pictures on a final fluorescent screen seems to be rather attractive. Picture multipliers of this sort have actually been constructed (C. 1). However, there are still great difficulties to overcome. The chromatic aberration which might be tolerable for the above picture transformer in many cases will spoil the definition of a picture very soon if repeated projection of the image is carried out. This chromatic aberration is particularly large for any multiplier, since the initial velocities of secondary electrons ($A V$ in eq. 7-4) are considerably larger than those of the photoelectrons which are projected on to the screen of the ordinary picture transformer. But apart from this fundamental difficulty there is still a long way to go before the optics of these extremely important amplifiers can be developed to a technically satisfactory standard.

VIII. Appendix

THE USE OF FIELDS WITH CYLINDRICAL SYMMETRY

In the previous chapters, electron lenses with rotational symmetry were alone considered. Fields of cylindrical symmetry are however used to a large extent in valves, electron multipliers, X-ray tubes with line focus, and in some cathode-ray tube constructions, for instance, those which are employed for sound-film recording, etc. These problems of cylindrical electron optics are treated here in an appendix only, but this seems justified, because little is known yet about cylindrical electron lenses and because the peculiarities of devices using cylindrically symmetrical fields can be explained better on an electron-mechanical than on an electron-optical basis.

On the other hand, it should not be forgotten that about ten years ago the optics of electron lenses with rotational symmetry was as little understood as is that of lenses with cylindrical symmetry to-day, so that the possibility of a substantial development of the electron optics of cylindrical fields must not be overlooked.

Inspection of the variety of possible electrostatic cylindrical-optical lenses reveals two main constructional elements, the slotted diaphragm and the double plate. These elements correspond respectively to the circular diaphragm and the tube of rotationally symmetrical electron optics. For instance, in cylinder optics, the cross-sections of the lenses in Fig. 4-3 *b. c* and *d* would belong to different types of four-plate lenses, the cross-sections in Fig. 4-3 *e, f* and *g* would be examples of cylinder optical electron lenses using plates and slot diaphragms. In order to provide fields of real cylindrical symmetry, a sufficiently large extension of the electrodes in the direction perpendicular to the plane of Fig. 4-3 has to be secured.

Some information on the field distribution of some simple cylindrical optical arrangements can be obtained from the papers of A. Glaser and W. Henneberg (G. 3) and of T. C. Fry (F. 3). Comparing a spherical and a cylindrical electron lens, both having exactly the same cross-section of the electrodes and both using the same voltage ratio, the following may be expected. The lens with cylindrical symmetry should have a shorter focal length than that with rotational symmetry, because the electric fields penetrate to a larger extent through the arrangement with cylindrical symmetry. The very few experimental results seem to confirm this opinion.

A short note has been published by C. J. Davisson and C. J. Calbick (D. 1) on a lens produced by a slotted diaphragm separating two spaces with different field strength E and E'. If V is the potential of the diaphragm, the approximate focal length of this lens is found to be

$$v$$

the sign of f depending upon the relative intensity of the fields E and E'. Fig. 8-i shows the simple arrangement which was used by Davisson and Calbick. A thin filament F is surrounded by two coaxial, slotted cylinders A and B. Because of the logarithmic decay of the potential near the thin filament, the field E on the inside and

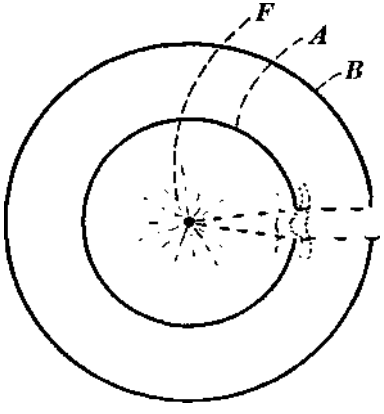

Fig. 8-i. Focusing by a slot.

close to the first cylinder A can be assumed to be approximately zero $(E = o)$. The field E' at the outside and close to this cylinder A is found from the potential difference and the distance between the two cylinders A and B. If the potentials are chosen in such a manner that the beams leaving the cylinders are parallel, then the filament F must be at the focus of cylinder A. The formula (8-i) holds sufficiently accurately if the diameters of the two cylinders are both large in comparison with the width of the slot. In this way the cylindrical surfaces approximate to two infinite planes. In this connection, it is of some interest to note, that if the slots in the cylinders are replaced by circular apertures of the same cross-sectional width, the factor 2 in the formula (8-i) must be replaced by a factor 4, so that, in this case, the lens with rotational symmetry has just twice the focal length of the corresponding lens with cylindrical symmetry.

The most promising field for the application of cylindrical electron optics is at present found in the problems of valve technique. M. Knoll (K. 6) has given a detailed discussion of the bunching action of the control grids in valves. Fig. 8-2 shows the field plot of a plane electrode-arrangement with some electron paths which were estimated by a rough ray tracing through the equipotentials measured in the electrolytic trough. Seven different pictures are shown in this figure, corresponding to conditions of different grid bias. If the voltage ratio between grid and anode is about equal to the ratio of distances from grid to anode and from cathode to anode, hardly any lens action will occur. If (going from the right to the left in the figure)

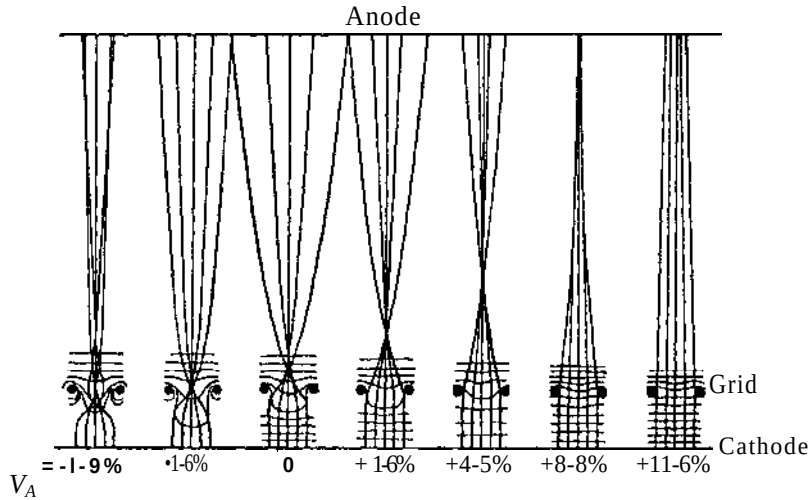

Fig. 8-2. Paths of electrons in a grid controlled triode, for different voltage ratios V_g/V_a between grid and anode.

this voltage ratio decreases, the focal length of the elementary lens decreases and the electrons are focused near the anode. For still smaller voltage ratio the electron paths cross over and a widely distributed spray is produced at the anode. Proceeding to negative voltage ratios, the power of the elementary lens becomes still larger and the beams are once more concentrated. Finally, for still more negative grid bias a second cross-over of the electron beams will be produced.

For triode valves these electron optical considerations might seem to be superfluous, since the characteristic valves can be calculated with a high degree of accuracy without any knowledge of the paths of the electrons. On the other hand, the study and the control of electron paths in multielectrode valves has already produced some

encouraging results. I. Shoenberg, C. S. Bull and S. Rodda (S. 5) first recommended a proper alignment of the grids. Later, M. Knoll (K. 6) has shown that the characteristic of a screen grid tetrode is improved if the screen is properly aligned with respect to the grid. In this case the screen current could be reduced by a factor 10 and the slope of the grid characteristic improved by a factor 2.

Moreover, I. Shoenberg, C. S. Bull and S. Rodda (S. 5) realised very early that a pentode power valve can be replaced by a tetrode with similar characteristics if the electrodes are properly shaped in order to produce a confined electron beam building up a space charge

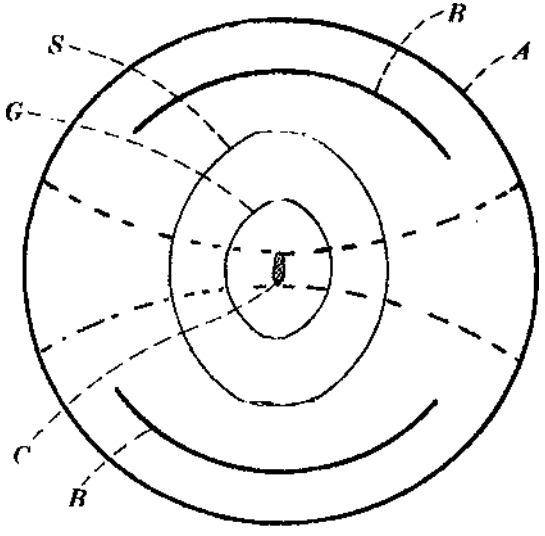

Fig. 83. Beam power valve.

region near the anode. A very thorough description of this "beam power valve" and its performance has been given recently by O. Schade (S. 1). As shown in the cross-section given in Fig. 8-3, the valve consists of a ribbon-shaped, indirectly heated cathode C, a control grid *G* of oval cross-section, a screen grid *S* also of oval cross-section at about 250 volts with respect to the cathode, an anode or plate electrode *A* at about 50 volts with respect to the cathode and of two beam-forming plates *B* which are at cathode potential and can therefore be considered as parts of the cathode. The electron current is formed into a beam, as indicated by the dotted lines in Fig. 8-3. This beam is confined to a sector by the two beam-forming plates at cathode potential. Moreover, as a space of relatively low potential is produced by these beam-forming plates, the electrons of the beam

are slowed down and a space charge is formed which stops the secondary electrons coming from the anode.

The current within the two above-mentioned sectors is also subdivided by the individual grid wires into directed beams of disc sector shape. This can be understood as follows. The grid and screen (*G* and *S* in Fig. 8-3) consist of wires extending parallel to the plane of the drawing, so that if the resultant field in the control grid plane is positive, electrons leave the space-charge-cloud at the cathode and are focused into disc-shaped sectors, the discs lying parallel to the plane of the drawing of Fig. 8-3. The voltage of the control grid governs the divergence of these disc-shaped beams. If the screen-grid is properly aligned, it is scarcely struck by the electron beams, so that the screen current can be reduced in this way to less than 2% of the anode current.

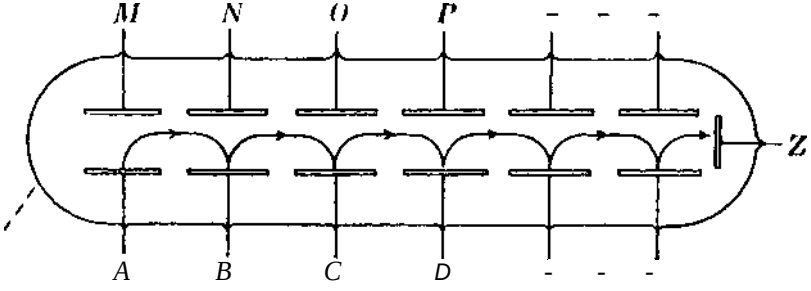

Fig. 84. Electric magnetic electron multiplier.

Beam valves replacing pentodes seem to be suitable for operation as class-A amplifiers, having substantially second harmonic distortion only and capable of high power output, high efficiency and high power sensitivity. Moreover, beam valves seem to provide large opportunities when used at the input side of an amplifier. It appears that the valve noise which is due to fluctuations of the electron current (shot effect, flicker effect, etc.) can be largely reduced in multielectrode valves, if the electron current is prevented by proper focusing from striking the screen and other auxiliary electrodes. The noise of the input valve is of greatest importance, since —in the absence of interference—it limits the least signal strength which can be received. A large amount of research has been done on the noise problem in recent years, but we must refrain here from quoting the voluminous literature on this subject since it would lead too far away from oar proper theme. It should, however, be emphasised that further progress by electron-optical methods will probably be most helpful in the line of valve development.

We must refrain from going into details about other devices using cylindrically symmetrical fields, but an important application of cylindrical optics to the construction of electron multipliers should be pointed out here as a particular example. The magnetic electric multiplier (Z. 2, Z. 3) shown in Fig. 8-4 contains two rows of plane electrodes in a tube T, those in the bottom row *B*, C, D, ... are secondary emitters, while those in the upper row M_y *N*, O, P, ... serve to maintain a transverse electrostatic field between the two sets of electrodes. Each target in the bottom row is made positive with respect to the preceding one. A magnetic field is established perpendicular to the axis of the tube and to the field between the two rows of plates. Electrons leaving the cathode *A* are bent by the combined fields in such a way that they strike the target *B*. They release there secondary electrons which are in turn deflected to the plate *B*, the secondaries from *B* will strike the target *C* and the multiplication will go on in this manner through the tube. The final output is collected at the electrode *Z*. Multipliers of this sort have to be used with sufficiently small input, since the current density which the sensitised plates can stand is rather limited. If, however, the input currents are sufficiently small, amazing amplifications can be obtained. For instance, tubes such as that of Fig. 8-3 have been constructed using up to twelve stages, and current amplifications of several million times have been obtained with them. This successful performance illustrates that the application of cylindrically symmetrical fields may, in some cases, offer an definite advantage over a corresponding construction using electron lenses with rotational symmetry.

LITERATURE

For a further study of electron optics, the excellent book by E. Briiche and O. Scherzer (B. II) may be recommended. The author has also been informed that there will appear shortly two other books on electron optics. W. Glaser will publish a detailed account of this subject from the theoretical point of view and I. G. Maloff and D. Epstein will deal with electron optical problems with a view mainly to their technical application in television.

For a detailed study of electron optics an accurate knowledge of the two fundamental subjects of electron physics and of light optics is essential, both subjects forming the basis of electron optics. For a study of electron physics reference may be made to the book of the present author (K. i). On the subject of geometrical optics, there exists an enormous multitude of elementary as well as of advanced books. The text books by A. C. Hardy and F. H. Perrin (H. i) and by P. Drude (D. 6) are very suitable for a general study of the applied and of the theoretical optics respectively. The standard work by A. E. Conrady (C. 2) may be recommended as a comprehensive survey on all problems of optical design.

A. 1. M. v. Ardenne, *Zeits. Physik* ,**108,** 338, 1938.

B. 1. L. H. Bedford, *Journ. Scient. Instr.* 13, 177, 1936.
B. 2. M. Born, *Optik.* Berlin, 1933.
B. 3. B. von Borries and E. Ruska, *Wiss. Veroff. Siemens,* 17, 99, 1938.
B. 4. A. Bouwers, *Physica,* 2, 148, 1935.
B. 5. A. Bouwers, *Physica,* 4, 200, 1937.
B. 6. E. Briiche and W. Henneberg, *Erg. exact. Natw.* 15, 365, 1936.
B. 7. E. Briiche and H. Johannson, *Naturw.* 20, 49 and 353, 1932.
B. 8. E. Briiche and H. Johannson, *Zeits. techn. Physik,* 14, 487, 1933.
B. 9. E. Briiche and W. Knecht, *Zeits. techn. Physik,* 15, 461, 1934 and 16, 95, 1935.
B. 10. E. Briiche and H. Mahl, *Zeits. techn. Physik,* 17, 81 and 262, 1936.
B. 11, E. Briiche and O. Scherzer, *Geometrische Elektronenoptik.* Berlin, 1934.
B. 12. W. G. Burgers and J. P. van Amstel, *Physica,* 4, 5 and 15, 1937 and 5, 305 and 313, 1938
B. 13. H. Busch, *Ann. Physik,* **81,** 974, 1926; *Arch. ElektroU* **18,** 583, **1927.**
B. 14. H. Busch and E. Briiche, *Beitrdge zur Elektronenoptik.* Leipzig, 1937.

C. 1. F. Coeterier and M. C. Teves, *Physica,* 4, 33, 1937.
C. 2. A. E. Conrady, *Applied Optics and Optical design.* Oxford, 1929.
C. 3. C. R. Cosens, *Proc. Phys. Soc. Lond.* 46, 818, 1934.

D. 1. C. J. Davisson and C. J. Calbick, *Phys. Rev.* **38,** 585, 1931 and *42,* 58o, 1932.
D. 2. K. Diels and M. Knoll, *Zeits. techn. Physik,* **16,** 617, 1935.
D. 3. K. Diels and G. Wendt, *Zeits. techn. Physik,* **18,** 65, 1937.
D. 4. J. Dosse, *Zeits. techn. Physik,* 17, 315, 1936.
D. 5. E. Driest and H. Muller, *Zeits. wiss. Mikrosk,* 52, 53, 1935.
D. 6. P. Drude, *Theory of Optics.* Translation by R. A. Millikan. London, 1902.

E. 1. D. W. Epstein, *Proc. Inst. Rad. Eng.* 24, 1095, 1936.

F. 1. P. T. Farnsworth, *Journ. Franklin Inst.* **218,** 411, 1934.
F. 2. Ferranti Ltd. and M. K. Taylor, British Patent No. 472, 165. I936-7-
F. 3. T. C. Fry, *Bell Tel. Syst.* Math. Phys. Monogr. No. B 671.

G. 1. D. Gabor, *Nature,* **139,** 373, 1937.
G. 2. W. Glaser, *Zeits. Physik,* **80,** 451; **81,** 649; **83,** 104, 1933 and 97, 177, 1935-
G. 3. A. Glaser and W. Henneberg, *Zeits. techn. Physik,* **16,** 229, 1935.

H. 1. A. C. Hardy and F. H. Perrin, *The Principles of Optics.* New York and London, 1932.
H. 2. W. Heimann, *El. Nachr. Tech.* **12,** 68, 1935.
H. 3. W. Heinze and S. Wagener, *Zeits. techn. Physik,* 17, 645, 1936.
H. 4. W. Henneberg and A. Recknagel, *Zeits. techn. Physik,* 16, 230, 1935-
H. 5. W. Henneberg and A. Recknagel, *Zeits. techn. Physik,* 16, 621, 1935.
H. 6. E. Hess, *Zeits. Physik,* **92,** 274, 1934.
H. 7. G. Hottenroth, *Zeits. Physik,* **103,** 460, 1936; *Ann. Physik,* 30, 689, 1937.
H. 8. J. V. Hughes, *Phil. Mag.* **19,** 129, 1935.

J. 1. H. Johannson, *Ann. Physik,* **18,** 385, 1933 and **21,** 275, 1934.
J. 2. H. Johannson and O. Scherzer, *Zeits. Physik,* **80,** 183, 1933.

K. 1. O. Klemperer, *Einfuhrung in die Elektronik.* Berlin, 1933.
K. 2. O. Klemperer, *Phil. Mag.* **20,** 545, 1935.
K. 3. O. Klemperer and W. D. Wright, *Proc. Roy. Soc.* **166,** 58, Abstr., 1938 and *Proc. Phys. Soc.* In course of publication.
K. 4. W. Knecht, *Ann. Physik,* **20,** 161, 1934.
K. 5. M. Knoll and E. Ruska, *Zeits. techn. Physik,* **12,** 394, 1931; *Ann. Physik,* **12,** 607 and 641, 1932; *Zeits. Physik,* 78, 318, 1932.
K. 6. M. Knoll, *Zeits. Techn. Physik,* 15, 584, 1934.
K. 7. F. Krause, *Zeits. Physik,* **102,** 417, 1936.
K. 8. F. Krause, *Naturw.* 25, 817, 1937 and **26,** 122, 1938.

L. 1. D. B. Langmuir, *Nature,* **139,** 1067, 1937.
L. 2, D. B. Langmuir, *Proc. Inst. Rad. Eng. 2$,* 977, 1937.
L. 3. R. R. Law, *Proc. Inst. Rad. Eng.* 25, 954, 1937.
L. 4. G. Lubszynski and S. Rodda, British Patent No. 442,666. 1934-6.

M. i. I. G. Maloff and D. W. Epstein, *Proc. Inst. Rad. Eng.* **22,** 1386, 1934.
M. 2. M. B. Manifold and F. N. Nicoll. *Nature,* **142,** 39, 1938.
M. 3. L. C. Martin, R. V. Welpton and D. H. Parnum, *Journ. Scient. Instr.* **14,** 14, 1937.
M. 4. I. D. McGee and G. Lubszynski, *Proc. Inst. El. Eng.* In course of publication. 1938.
M. 5. L. Marton, *Nature,* **133,** 911, 1934; *Revue optique,* **14,** 129, 1935; *Physica,* 3, 959, 1936; *Bull. d. Belg.* **22,** 1336, 1936.
M. 6. G. A. Morton and E. G. Romberg, *Physics,* 7, 451, 1936.

N. 1. F. H. Nicoll, *Proc. Phys. Soc.* **50,** 888, 1938.

O. 1. F. Ollendorf and G. Wendt, *Zeits. Physik,* 76, 655, 1932.

P. 1. J. Picht, *Ann. Physik,* **15,** 926, 1932.
P. 2. Physical Society, *Report on teaching of geometrical optics.* London 1934. Referring to the proposed two sign conventions, for the purpose of an elementary discussion of electron optical problems, it seems preferable to refrain from using a Cartesian frame work.

R. 1. A. Recknagel, *Zeits. Physik,* **104,** 381, 1937.
R. 2. W. Rogowski, *Archiv f. El.* **31,** 555, 1937.
R. 3. E. Ruska, *Zeits. Physik,* 83, 684, 1933.
R. 4. E. Ruska, *Zeits. Physik,* 87, 580 and 89, 90, 1934.

S. 1. W. Schaffernicht, *Zeits. techn. Physik,* **17,** 596, 1936.
S. 2. T. Schlomka, *Zeits. techn. Physik,* **17,** 459, 1936.
S. 3. O. Schade, *Proc. Inst. Rad. Eng.* 26, 137, 1938.
S. 4. I. Shoenberg, G. E. Condliffe and W. F. Tedham, British Patent, No. 431,327. I933~5,s,5
S. 5. I. Shoenberg, C. S. Bull and S. Rodda, British Patent No. 423,932. 1933-5.
S. 6. C. Stormer, *Ann. Physik,* 16, 685, 1933.
S. 7. J. L. Synge, *Geometrical Optics.* Cambridge tracts, No. 37. 1937-

W. 1. E. E. Watson, *Phil. Mag.* 3, 849, 1927.
W. 2. W. D. Wright and O. Klemperer, British Patent No. 480,857. 1936-8.

Z. 1. V. K. Zworykin, *Journ. Inst. El. Eng.* **73,** 437, 1933; *Journ. Franklin Inst.* **215,** 535, 1933 and **217,** 1, 1934.
Z. 2. V. K. Zworykin, *Journ. Inst. El. Eng.* 79, 1, 1936.
Z. 3. V. K. Zworykin, G. A. Morton and L. Malter, *Proc. Inst. Rad. Eng.* **24,** 351, 1936.

INDEX